

## **DETECTION OF BURIED OBJECTS IN A TWO LAYER MEDIUM ILLUMINATED BY A DIPOLE**

R. H. Ott

GRCI, Inc.

SWL Div.

3900 Juan Tabo Blvd.

NE Suite 12 Albuquerque, NM 87111-3984

- 1. Introduction**
  - 2. Target Illuminated by a Vertical Magnetic Dipole (VMD) in Region (1)**
    - 2.1 Unperturbed Fields in Region (1)
    - 2.2 Unperturbed Fields in Region (2)
    - 2.3 Scattered Fields
  - 3. Quasi-Static Fields in Terms of Induced Dipole Moments**
  - 4. Polarizability**
    - 4.1 Sphere
    - 4.2 Polarizability of an Ellipsoid
  - 5. Scattered Fields in Region (1) for a VMD in Region (1)**
    - 5.1 Theory
    - 5.2 Examples
  - 6. Scattered Fields in Region (1) for a Horizontal Magnetic Dipole (HMD) in Region (1)**
    - 6.1 Theory
    - 6.2 Example
  - 7. Scattered Fields in Region (1) for a VED in Region (1)**
  - 8. Scattered Fields in Region (1) for a HED in Region (1)**
  - 9. Metal Detector Analysis**
- References**

## 1. INTRODUCTION

The geometry for the dipole source, the layered medium, the target and observer are shown in figure 1. An electrically small dipole source is located at the origin of a  $x, y, z$ -coordinate system.

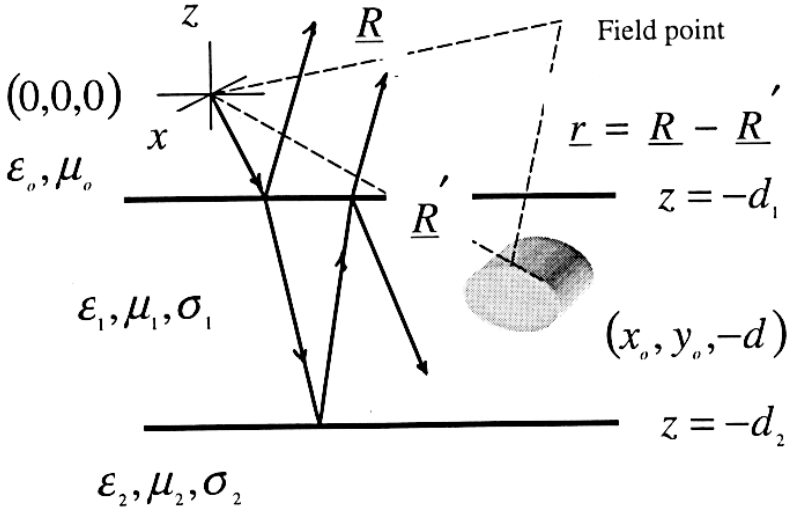


**Figure 1.** Geometry for a dipole source above a layered medium containing a target.

The electric and magnetic fields of a dipole source can be calculated from the respective electric and magnetic Hertz potentials as

$$\begin{aligned}
 \underline{\mathbf{E}} &= \frac{1}{-i\omega\epsilon} \nabla \times \nabla \times \underline{\pi}^e \\
 \underline{\mathbf{H}} &= \nabla \times \underline{\pi}^e \\
 \underline{\mathbf{H}} &= \frac{1}{i\omega\mu} \nabla \times \nabla \times \underline{\pi}^m \\
 \underline{\mathbf{E}} &= \nabla \times \underline{\pi}^m
 \end{aligned} \tag{1}$$

where the electric ( $\underline{\pi}^e$ ) and magnetic ( $\underline{\pi}^m$ ) Hertz potentials are

represented by the Sommerfeld identity

$$\begin{aligned}
 \pi_m^e &= \frac{e^{ik|\mathbf{R}-\mathbf{R}'|}}{4\pi|\mathbf{R}-\mathbf{R}'|} \\
 &= \frac{i}{4\pi} \sum_{m=-\infty}^{\infty} e^{im(\phi-\phi')} \int_0^{\infty} J_m(k\rho) J_m(k\rho') e^{ik_z|z-z'|} \frac{k_\rho}{k_z} dk_\rho \\
 &\quad k_z = \pm \sqrt{k^2 - k_\rho^2} \\
 \pi &= \begin{cases} -i\omega\mu m\pi^m, & \text{magnetic dipole} \\ -i\omega p\pi^e, & \text{electric dipole} \end{cases} \\
 \nabla \times \nabla \times \underline{\pi}^e - \nabla \nabla \cdot \underline{\pi}^e - k^2 \underline{\pi}^e + i\omega\mu\sigma \underline{\pi}^e &= 0
 \end{aligned} \tag{2}$$

and  $\mathbf{R}, \mathbf{R}'$  are shown in figure 1. Using the addition theorem for cylindrical Bessel functions from Abramowitz and Stegun, (1965, page 363) equation (2) becomes

$$\begin{aligned}
 \pi_m^e &= \frac{e^{ik|\mathbf{R}-\mathbf{R}'|}}{4\pi|\mathbf{R}-\mathbf{R}'|} \\
 &= \frac{i}{4\pi} \int_0^{\infty} J_0\left(\left|\underline{\rho}-\underline{\rho}'\right|\right) e^{ik_z|z-z'|} \frac{k_\rho}{k_z} dk_\rho \\
 &= \frac{1}{4\pi r}, \text{ quasi-static}
 \end{aligned} \tag{3}$$

It is instructive to compare the Sommerfeld Hertzian potential approach (Sommerfeld, 1949, Wait, 1951, Banos, 1966) to the ‘‘propagation matrix approach’’, (with constraints, Chew, 1995, and without constraints, Kong, 1972). The potential approach starts with the following expression for the scattered potential in region (1) ( $e^{i\omega t}$  time convention);

$$\phi_1^s = \left(\frac{1}{4\pi}\right) \left(\frac{Il}{-i\omega\varepsilon_0}\right) \int_0^{\infty} R(\lambda) J_0(\lambda\rho) e^{-ik_z(z+d_1)} \frac{\lambda d\lambda}{-ik_z} \tag{4}$$

and the following expression for the scattered potential in region (2),

$$\phi_2^s = \left(\frac{1}{4\pi}\right) \left(\frac{Il}{-i\omega\varepsilon_0}\right) \int_0^{\infty} T(\lambda) J_0(\lambda\rho) e^{-ik_{2z}z+k_{1z}d_1} \frac{\lambda d\lambda}{-ik_{1z}} \tag{5}$$

where,

$$\begin{aligned} k_{1z} &= \sqrt{k_0^2 - \lambda^2} \cong i\lambda \\ k_{2z} &= \sqrt{k_2^2 - \lambda^2} \\ k_2 &= k_0^2 \left( \varepsilon_{r1} + \frac{i\sigma_1}{\omega\varepsilon_0} \right) \end{aligned} \quad (6)$$

The boundary conditions on tangential  $\underline{\mathbf{E}}$  and  $\underline{\mathbf{H}}$  (because of azimuth symmetry only  $\underline{\mathbf{E}}_\rho$  and  $\underline{\mathbf{H}}_\phi$ ) require the scattered potentials in regions (1) and (2) to satisfy

$$\begin{aligned} \frac{\partial \phi_1^s}{\partial z} \Big|_{z=0} &= \frac{\partial \phi_2^s}{\partial z} \Big|_{z=0} \\ \phi_1^s &= n^2 \phi_2^s \end{aligned} \quad (7)$$

which in turn yield the following results for the reflection and transmission coefficients

$$\begin{aligned} R(\lambda) &= \frac{n^2 k_{1z} - k_{2z}}{n^2 k_{1z} + k_{2z}} \\ T(\lambda) &= \frac{2k_{1z}}{n^2 k_{1z} + k_{2z}} \end{aligned} \quad (8)$$

where Frazer-Smith (1987) makes the following additional approximation in the denominators of equation (8)

$$n^2 k_{1z} = \left( \varepsilon_{r2} + \frac{i\sigma_1}{\omega\varepsilon_0} \right) (i\lambda) \cong -\frac{\sigma_1}{\omega\varepsilon_0} \lambda \quad (9)$$

Further, to obtain the Frazer-Smith result, the following approximations are required in the denominators of equation (8)

$$R(\lambda) \cong 1 \quad (10)$$

$\sigma_1 \rightarrow \infty$

Substituting (6) and (9) into (4) gives

$$\phi_1^s = \frac{Il}{2\pi\sigma_1} \int_0^\infty J_0(\lambda\rho) e^{-\sqrt{\lambda^2 - k_{2z}^2}z - \lambda d_1} \frac{\lambda d\lambda}{-ik_{1z}} \quad (11)$$

The result in equation (11) assumes no lower boundary to simplify the comparison with the “propagation matrix approach”. This assumption results in the following approximation in the Frazer-Smith result

$$F_{1M} = \frac{1 + \frac{Y_{-1}-Y_0}{Y_{-1}+Y_0} e^{2\sqrt{\lambda^2-k_2^2}(z-d_2)}}{1 - \left(\frac{Y_{-1}-Y_0}{Y_{-1}+Y_0}\right) \left(\frac{Y_1-Y_0}{Y_1+Y_0}\right) e^{\sqrt{\lambda^2-k_2^2}d_2}} \xrightarrow{d_2 \rightarrow \infty} 1 \quad (12)$$

Then the vertical component of the magnetic field is

$$\begin{aligned} H_{1z} &= \left( \frac{\partial^2}{\partial z^2} + k_1^2 \right) \phi_1^s \\ &= \left( \frac{1}{4\pi} \right) \left( \frac{Il}{-i\omega\varepsilon_0} \right) \int_0^\infty (-k_{1z}^2 + k_1^2) R(\lambda) J_0(\lambda\rho) e^{-ik_{1z}|z+d_1|} d\lambda \\ Il &\rightarrow -i\omega\mu_0 m, \quad m = IA \\ \varepsilon &\rightarrow -\mu_0 \\ \left( \frac{-i\omega\mu_0 m}{i\omega\mu_0} \right) \left( \frac{1}{-i4\pi} \right) &= \frac{-im}{4\pi} \\ H_{1z} &= \left( \frac{-im}{4\pi} \right) \int_0^\infty \frac{\lambda^3}{\sqrt{k_1^2 - \lambda^2}} J_0(\lambda\rho) e^{-\sqrt{k_{1z} - \lambda^2}|z+d_1|} d\lambda \end{aligned} \quad (13)$$

The Sommerfeld approach has the following limitations: 1) The distances are not necessarily small to a wavelength in the medium so that both electric and magnetic dipole moments need to be considered. 2) In order to insure higher order multipoles are not important, the maximum dimension of the underground object must be small compared to the geometric mean of the source and observer distances. 3) The maximum dimension of the buried object must be small compared to the distance between the object and the interface so that higher order interactions are not important. It is important to note that the Plane-Wave Scattering Matrix formulation (Kern, 1981, a spectral approach to the various field quantities) would overcome all three of these restrictions; however, the mathematical derivation for the Plane-Wave formulation at present has not been derived for the case of three layers. The two interface case with a buried target has been treated by Ott (1996) (Three interface, two region case with a buried object has been submitted for publication, Ott, 1998). In general, the Sommerfeld formulation is equivalent to the Plane-Wave Scattering Matrix

formulation except the double integrals over  $\underline{k}_x, \underline{k}_y$  space are cast into polar form with the  $\phi$ -integration performed analytically and generating the Bessel functions as above. In cases where the scattered near fields are needed, and the receiving antenna is located near the interface, the Plane-Wave Scattering Matrix formulation can be evaluated numerically by a two-dimensional fast Fourier transform over a grid of field values at discrete values of  $(x, y)$ . Both formulations have the potential of including near field effects. The advantage of the Sommerfeld approach is its easy generalization of objects of different shapes in terms of their polarizabilities. In the Plane-Wave Scattering Matrix approach, the scattered fields from the objects are calculated using a Born scattering approximation.

The propagation matrix approach for the vertical component of the magnetic field for magnetic dipole above a layered medium is (Chew, 1995)

$$H_{1z}(\rho, z) = \left( \frac{-im}{4\pi} \right) \int_0^\infty \frac{k_\rho^3}{\sqrt{k_1^2 - k_\rho^2}} J_0(\lambda\rho) \left[ e^{-k_{1z}|z|} + \tilde{R}_{12}^{TE} e^{ik_{1z}z + 2ik_{1z}d_1} \right] dk_\rho \quad (14)$$

where the  $2^{nd}$  term in brackets is the scattered field from the interface as in (13) when the approximation in (10)  $\tilde{R}_{12}^{TE} \rightarrow 1$  is made. Also, the origin for the Frazer-Smith result is at the interface, while the origin for the Chew result is at the dipole, accounting for the factor of 2 in (14).

This paper derives the fields scattered in the upper layer by a buried target in the middle layer, for all possible polarizations of the incident field in the upper layer. All possible combinations of polarization for the induced dipole moment of the scatterer in the middle layer of a 3-layer medium are considered. Some published results are available for a single incident polarization (e.g. **VMD**, **VED**) in a 2-layer medium. Also, the quasi-static approximations for all polarization cases are derived.

## 2. TARGET ILLUMINATED BY A VERTICAL MAGNETIC DIPOLE (VMD) in REGION (1)

### 2.1 Unperturbed Fields in Region (1)

In the “propagation matrix approach”, tangential  $\underline{\mathbf{E}}$  and  $\underline{\mathbf{H}}$  are continuous across each interface and in addition, Chew (1995) includes the extra phase factor  $e^{2ik_{1z}d}$  to insure  $\mathbf{R}(\mathbf{k}_\rho)$  and  $\mathbf{T}(\mathbf{k}_\rho)$  are properly defined as reflection and transmission coefficients.

Although the distances in our problem are much less than the free-space wavelength, they are not necessarily small to a wavelength in region (2). Consequently, the induced electric dipole moment and the induced magnetic dipole moment must be considered. Since both type of dipole moments are induced, both the unperturbed electric and magnetic fields at the target center  $(x', y', z') = (x_0, y_0, -d)$  must be derived. The unperturbed fields involve both  $z$ -and transverse components. In general, in any region, the transverse components can be obtained from the  $z$ -component using (Chew, 1995) the following results (for the integrands of the fields):

$$\begin{aligned}\underline{\mathbf{E}}_t &= \frac{1}{k_\rho^2} \begin{pmatrix} \left( \underline{\epsilon}_\rho \frac{\partial}{\partial \rho} + \frac{\epsilon_\phi}{\rho} \frac{\partial}{\partial \phi} \right) \left( \frac{\partial E_z}{\partial z} \right) \\ -i\omega\mu\underline{\epsilon}_z \times \left( \underline{\epsilon}_\rho \frac{\partial}{\partial \rho} + \frac{\epsilon_\phi}{\rho} \frac{\partial}{\partial \phi} \right) H_z \end{pmatrix} \\ \underline{\mathbf{H}}_t &= \frac{1}{k_\rho^2} \begin{pmatrix} \left( \underline{\epsilon}_\rho \frac{\partial}{\partial \rho} + \frac{\epsilon_\phi}{\rho} \frac{\partial}{\partial \phi} \right) \left( \frac{\partial H_z}{\partial z} \right) \\ i\omega\varepsilon\underline{\epsilon}_z \times \left( \underline{\epsilon}_\rho \frac{\partial}{\partial \rho} + \frac{\epsilon_\phi}{\rho} \frac{\partial}{\partial \phi} \right) E_z \end{pmatrix}\end{aligned}\quad (15)$$

The  $z$ -component of the unperturbed field in region (1) is given in (14); however, we derive it here for completeness rather than quoting Chew’s result.

From equations (1), (2) and (3) we have, for the unperturbed  $z$ -component of the magnetic field in region 1:

$$\begin{aligned}H_z(\rho, z) &= \frac{1}{-i\omega\mu_0} (-i\omega\mu_0 m_z) \left( \frac{\partial^2}{\partial z^2} + k_1^2 \right) \pi_z^m \\ &= m_z \frac{-i}{4\pi} \left( k_1^2 \pi_z^m + \int_0^\infty \frac{k_\rho}{k_{1z}} J_0(k_\rho |\underline{\rho} - \underline{\rho}'|) \frac{\partial^2}{\partial z^2} e^{ik_{1z}|z-z'|} dk_\rho \right)\end{aligned}$$

$$\begin{aligned}
&= \frac{-im_z}{4\pi} \int_0^\infty \frac{k_\rho}{k_{1z}} J_0(k_\rho|\underline{\rho} - \underline{\rho}'|) (k_1^2 - k_z^2) e^{ik_{1z}|z-z'|} dk_\rho \\
&= \frac{-im_z}{4\pi} \int_0^\infty \frac{k_\rho^3}{k_{1z}} J_0(k_\rho|\underline{\rho} - \underline{\rho}'|) e^{ik_{1z}|z-z'|} dk_\rho \tag{16}
\end{aligned}$$

From equation (15), the unperturbed transverse components of the magnetic field in region (1) are:

$$\begin{aligned}
\underline{\mathbf{H}}_t &= \underline{e}_\rho \frac{1}{k^2} \frac{\partial^2 H_z}{\partial \rho \partial z} \\
&= \underline{e}_\rho \left( \frac{-im_z}{4\pi} \right) \int_0^\infty \frac{1}{k_\rho^2} \frac{k_\rho^3}{k_{1z}} \frac{\partial}{\partial \rho} \{ J_0(k_\rho|\underline{\rho} - \underline{\rho}'|) \} \frac{\partial}{\partial z} e^{ik_{1z}|z-z'|} dk_\rho \\
&= \underline{e}_\rho \left( \frac{-im_z}{4\pi} \right) (-)(i) \int_0^\infty k_\rho^2 J_1(k_\rho|\underline{\rho} - \underline{\rho}'|) e^{ik_{1z}|z-z'|} dk_\rho \\
&= \left( \frac{-m_z}{4\pi} \right) (\underline{e}_x \cos \phi + \underline{e}_y \sin \phi) \int_0^\infty k_\rho^2 J_1(k_\rho|\underline{\rho} - \underline{\rho}'|) e^{ik_{1z}|z-z'|} dk_\rho \tag{17}
\end{aligned}$$

Including the reflection from the interface, the  $\rho$ -component of the unperturbed field in region (1) is, from equations (14) and (15),

$$\begin{aligned}
H_{1\rho}^{unpert}(\rho, z) &= \left( \frac{-m_z}{4\pi} \right) \int_0^\infty k_\rho^2 J_1(k_\rho|\underline{\rho} - \underline{\rho}'|) \\
&\quad \cdot \left[ (\mp) e^{ik_{1z}|z-z'|} + \tilde{R}_{12}^{TE} e^{ik_{1z}(z-z')+2ik_{1z}} \right] dk_\rho \tag{18}
\end{aligned}$$

In order to compare the result in equation (18) with Kong (1972), the following replacements for the current moments are necessary in Kong's expressions,

$$Il \rightarrow \begin{cases} -i\omega p, & \text{electric dipole} \\ -i\omega\mu m, & m = IA = \text{magnetic dipole moment} \end{cases} \tag{19}$$

If the replacements in (19) are made in equation (36b), page 992, Kong (1972), equation (18) agrees with Kong's result. A similar comparison shows agreement for  $\mathbf{E}_{1\phi}^{unpert}$  and equation (36c), page 992, Kong.



An additional reason for using dipole moments versus current moments is in the following derivations involving the Sommerfeld identity for the fields in the various regions, in is more consistent to use the electric polarizability (dipole moment) for both the induced electric and magnetic dipole moments.

## 2.2 Unperturbed Fields in Region (2)

A **VMD** in region (1) produces a  $z$ -component (TE) field in region (2) given by (Chew, 1995)

$$H_{2z}^{\text{unpert}}(\rho, z) = \left( \frac{-im}{4\pi} \right) \int_0^{\infty} \frac{k_{\rho}^3}{k_{1z}} J_0(k_{\rho}|\rho - \rho'|) \cdot A_2^{TE} \left[ e^{-ik_{2z}(z-z')} + \tilde{R}_{23}^{TE} e^{i2k_{2z}d_2 + ik_{2z}(z-z')} \right] dk_{\rho} \quad (20)$$

where  $z < 0$ , since the field point is in region (2). In Barrick's (1995) notation

$$k_{2z} = i\sqrt{k_{\rho}^2 - k_2^2} = -\gamma_s \quad (21)$$

The propagation constants and wave-numbers in the various regions are given by

$$\begin{aligned} k_1^2 &= \omega^2 \varepsilon_0 \mu_0 \\ k_2^2 &= k_1^2 \left( \varepsilon_{r1} + \frac{i\sigma_1}{\omega \varepsilon_0} \right) \\ k_3^2 &= k_1^2 \left( \varepsilon_{r2} + \frac{i\sigma_2}{\omega \varepsilon_0} \right) \\ k_{1z} &= \sqrt{k_1^2 - k_{\rho}^2} \cong ik_{\rho} \\ k_{2z} &= \sqrt{k_2^2 - k_{\rho}^2} \cong i \left( k_{\rho} - \frac{k_2^2}{2k_{\rho}} \right) \\ k_{3z} &= \sqrt{k_3^2 - k_{\rho}^2} \cong i \left( k_{\rho} - \frac{k_3^2}{2k_{\rho}} \right) \end{aligned} \quad (22)$$

The reflection and transmission coefficients in equations (14) and (20) are given by ( $\mu_1 = \mu_2$ )

$$\tilde{R}_{12}^{TE} = R_{12}^{TE} + \frac{T_{12}^{TE} R_{23}^{TE} T_{21}^{TE} e^{2ik_{2z}(d_2-d_1)}}{1 - R_{21}^{TE} R_{23}^{TE} e^{2ik_{2z}(d_2-d_1)}}$$

$$\begin{aligned}
R_{12}^{TE} &= \frac{k_{1z} - k_{2z}}{k_{1z} + k_{2z}} \\
R_{23}^{TE} &= \frac{k_{2z} - k_{3z}}{k_{2z} + k_{3z}} \\
R_{21}^{TE} &= -R_{12}^{TE} \\
T_{21}^{TE} &= \frac{2k_{1z}}{k_{1z} + k_{2z}} \\
T_{21}^{TE} &= \frac{k_{2z}}{k_{1z}} T_{12}^{TE} \\
A_1 &= 1 \\
A_2^{TE} &= \frac{A_1 T_{12}^{TE} e^{i(k_{1z} - k_{2z})d_1}}{1 - R_{21}^{TE} R_{23}^{TE} e^{2ik_{2z}(d_2 - d_1)}}
\end{aligned} \tag{23}$$

The transverse components of the unperturbed field in region (2) are obtained by substituting (20) into (15) yielding the TE fields

$$\begin{aligned}
H_{2\rho}^{\text{unpert}}(\rho, z) &= \frac{-m}{4\pi} \int_0^\infty k_\rho^2 \frac{k_{2z}}{k_{1z}} J_1(k_\rho |\underline{\rho} - \underline{\rho}'|) \\
&\quad \cdot A_2^{TE} \left[ -e^{-ik_{2z}(z-z')} + R_{23}^{TE} e^{ik_{2z}(z-z') + 2ik_{2z}d_2} \right] dk_\rho \\
H_{2\phi}^{\text{unpert}}(\rho, z) &= 0 \\
E_{2\phi}^{\text{unpert}}(\rho, z) &= \frac{\omega\mu_0 m}{4\pi} \int_0^\infty \frac{k_\rho^2}{k_{1z}} J_1(k_\rho |\underline{\rho} - \underline{\rho}'|) \\
&\quad \cdot A_2^{TE} \left[ e^{-ik_{2z}(z-z')} + R_{23}^{TE} e^{ik_{2z}(z-z') + 2ik_{2z}d_2} \right] dk_\rho \\
E_{2\rho}^{\text{unpert}}(\rho, z) &= 0 \\
E_{2\rho}^{\text{unpert}}(\rho, z) &= 0(TE)
\end{aligned} \tag{24}$$

### 2.3 Scattered Fields

From the expressions for the induced electric and magnetic dipole moments in terms of the electric and magnetic polarizabilities, and the unperturbed electric and magnetic fields (the polarizabilities will be treated in the following section), it is possible to compute the scattered fields from the target. For the **VMD** case, by superposition,

the scattered magnetic fields can be written in terms of its rectangular components as the sum of the following three contributions,

$$\begin{aligned}
 H_x^s &= H_x^v + H_x^h + H_x^e \\
 H_y^s &= H_y^v + H_y^h + H_y^e \\
 H_z^s &= H_z^v + H_z^h + H_z^e
 \end{aligned} \tag{25}$$

where  $(H_x^v, H_y^v, H_z^v)$  are the reradiated fields for the induced vertical magnetic dipole moment,  $(H_x^h, H_y^h, H_z^h)$  are the reradiated fields for the induced horizontal magnetic dipole moment, and  $(H_x^e, H_y^e, H_z^e)$  are the reradiated fields for the induced electric dipole moment.

### 3. QUASI-STATIC FIELDS IN TERMS OF INDUCED DIPOLE MOMENTS

In a later section, an example will be considered as a demonstration of the accuracy of the quasi-static approach for the range of frequencies considered in this work (i.e., from 3 to 30 KHz). The  $z$ -component of the unperturbed magnetic field in region 1, is given in equation (16) and, using the approximations in equation (22) for  $k_{1z}$ , in the integrand of 16 we have

$$\begin{aligned}
 H_{1z}^{\text{unpert}}(\rho, z) &= \frac{im_z}{4\pi} \int_0^\infty \frac{k_\rho^3}{k_{1z}} J_0(k_\rho |\underline{\rho} - \underline{\rho}'|) e^{ik_{1z}|z-z'|} dk_\rho \\
 &\cong \frac{im_z}{4\pi} \int_0^\infty \frac{k_\rho^3}{ik_\rho} J_0(k_\rho |\underline{\rho} - \underline{\rho}'|) e^{ik_\rho|z-z'|} dk_\rho \\
 &= \frac{im_z}{4\pi} \frac{[2(z-z')^2 - (x-x')^2 - (y-y')^2]}{r^{\frac{5}{2}}} \\
 &= \frac{m_z}{4\pi r^{\frac{5}{2}}} [3(z-z')^2 - r^2] \\
 r &= \sqrt{(x-x')^2 + (y-y')^2 + (z-z')^2}
 \end{aligned} \tag{26}$$

In section 5, the induced electric and magnetic dipole moments are given as the product of the electric and/or magnetic polarizabilities and the unperturbed electric and magnetic fields. The resulting electric and magnetic fields reradiated to an observer, and these radiated fields will be evaluated using the above quasi-static approach. The

result in (26) can also be derived starting with the near-field spherical coordinate components for a small loop (Harrington, 1965), and recognizing that the quasi-static magnetic field does not depend on the medium properties; i.e., changes in  $\varepsilon$  or  $\mu$  across a boundary. This is exactly the reason a small loop is better for detecting buried objects than a vertical dipole. Using Harrington's result we have

$$\begin{aligned} H_\theta &= \frac{m}{4\pi r^3} \sin \theta \\ H_r &= \frac{m}{2\pi r^3} \cos \theta \end{aligned} \quad (27)$$

and converting these to rectangular coordinates gives

$$\begin{aligned} H_x &= \frac{3m_z xz}{4\pi r^5} \\ H_z &= \frac{m_z}{4\pi r^5} (3z^2 - r^5) \end{aligned} \quad (28)$$

in agreement with (26).

Similarly, the magnetic field of a  $x$ -directed electric dipole with

$$\pi_x = \frac{-\omega \varepsilon m}{4\pi r}$$

is

$$H_y = \frac{km}{4\pi r \eta_0}$$

## 4. POLARIZABILITY

### 4.1 Sphere

The magnetic field lines normal to a perfectly conducting sphere do not exist. However, in the plane perpendicular to the direction of the incident  $\mathbf{H}$  field loops currents are induced on the surface. These loop currents cancel the incident  $\mathbf{H}$  field, and in doing this satisfy the condition that the total normal  $\mathbf{H}$  is zero. It is useful to remember that the scattered magnetic dipole moment of a small sphere in free space is one-half the scattered electric dipole moment

The induced magnetic dipole moments for a spherical scatterer are (Wait, 1968)

$$\begin{aligned} m_x &= -2\pi a^3 [3(M - iN)] H_x^{unpert} \\ m_y &= -2\pi a^3 [3(M - iN)] H_y^{unpert} \\ m_z &= -2\pi a^3 [3(M - iN)] H_z^{unpert} \end{aligned} \quad (29)$$

where the unperturbed fields in (29) are evaluated at the target in figure 1  $(x', y', z') = (x_0, y_0, -d)$  in region (2). In equation (29) Wait shows

$$\begin{aligned} 3(M - iN) &= \\ &= \frac{2\mu_s(\sinh \alpha - \alpha \cosh \alpha) + \mu_0(\sinh \alpha - \alpha \cosh \alpha + \alpha^2 \sinh \alpha)}{\mu_s(\sinh \alpha - \alpha \cosh \alpha) - \mu_0(\sinh \alpha - \alpha \cosh \alpha + \alpha^2 \sinh \alpha)} \\ &\quad \alpha = \sqrt{-i\omega\mu_s\sigma_s a} \end{aligned} \quad (30)$$

and for a scatterer with free-space magnetic permeability, (30) reduces to

$$3(M - iN) = 1 + \frac{3(\sinh \alpha - \alpha \cosh \alpha)}{\alpha^2 \sinh \alpha} \quad (31)$$

$\mu_s = \mu_0$

Equation (30) has the high-frequency limit

$$\lim_{\alpha \rightarrow \infty} [3(M - iN)] = 1 \quad (32)$$

the low-frequency limits

$$\begin{aligned} 3(M - iN) &= 1 + \frac{3 \sinh \alpha - \alpha \cosh \alpha}{\alpha^2 \sinh \alpha} \\ &= 1 + \frac{3 \left( \alpha + \frac{\alpha^3}{3!} + \frac{\alpha^3}{5!} \right) - 3\alpha \left( 1 + \frac{\alpha^3}{2!} + \frac{\alpha^3}{4!} \right)}{\alpha^2 \left( \alpha + \frac{\alpha^3}{3!} + \frac{\alpha^3}{5!} \right)} \\ &= 1 + \frac{3\alpha + \frac{\alpha^3}{2} + \frac{\alpha^5}{40} - 3\alpha - \frac{3\alpha^3}{2} - \frac{\alpha^5}{8}}{\alpha^3 \left( 1 + \frac{\alpha^2}{6} \right)} \\ &= 1 + \frac{-\alpha^3 - \frac{\alpha^5}{10}}{\alpha^3 \left( 1 + \frac{\alpha^2}{6} \right)} \\ &= 1 - \left( 1 + \frac{\alpha^2}{10} \right) \left( 1 - \frac{\alpha^2}{6} \right) \\ &= \frac{\alpha^2}{15} \end{aligned} \quad (33)$$

If we assume  $\sigma_s \gg \sigma_1$  then the induced electric current moment is given by (Van de Hulst, 1957)

$$(Idl)_{\{x,y,z\}} = 4\pi\sigma_1 a^3 E_{\{x,y,z\}}^{unpert} \quad (34)$$

which is valid even if  $\alpha$  is not large (Wait, 1960). The electric current-moment has dimensions of current times length and differs by a factor  $-i\omega$  from the electric-dipole moment which has dimensions of charge times length; i.e.,

$$\begin{aligned} \underbrace{p_{\{x,y,z\}}}_{\substack{\text{electric} \\ \text{dipole} \\ \text{moment}}} &= \frac{(Idl)}{-i\omega} = \frac{4\pi\sigma_1 a^3}{-i\omega\epsilon_o} \epsilon_o E_{\{x,y,z\}}^{unpert} \\ &= 4\pi\hat{\epsilon} a^3 \epsilon_o E_{\{x,y,z\}}^{unpert} \\ \hat{\epsilon} &= \epsilon_{r1} + \frac{i\sigma_1}{\omega\epsilon_o} \quad (35) \\ p_{\{x,y,z\}} &\cong 4\pi \left( \frac{i\sigma_1}{\omega\epsilon_o} \right) a^3 \epsilon_o E_{\{x,y,z\}}^{unpert} \\ &= \alpha_e E_{\{x,y,z\}}^{unpert} \\ \alpha_e &= 4\pi a^3 \hat{\epsilon} \epsilon_o \end{aligned}$$

In equation (35) we note that the electric dipole moment  $p_{\{x,y,z\}}$  contains the factor  $\epsilon$ , while the magnetic dipole moment,  $m_{\{x,y,z\}}$  does not contain  $\mu$ .

Another method for obtaining the dipole-moment for buried scatterers is the Born approximation (Hill and Cavcey, 1988). This method is useful for the case of targets of arbitrary shape since the targets volume is included in the formulation. The method is best suited to a plane-wave spectrum (Kerns, 1981) representation for the incident fields on the scatterer. In contrast, our formulation represents the incident field as a Sommerfeld integral. For completeness, we show the Born approximation since it shows how to treat the case where the buried object is a dielectric or even a void in the layer. The Born approximation is valid even in the near-or far-field, but only for scatterers of small contrast to the surrounding medium. In the Born approximation the dipole-moment for a sphere is given by

$$\begin{aligned}
 p_{\{x,y,z\}} &= \varepsilon_o \int_V (\hat{\varepsilon} - 1) E_{\{x,y,z\}}(x', y', z') d\mathbf{r}' \\
 &= \varepsilon_o (\hat{\varepsilon} - 1) \frac{4\pi a^3}{3} E_{\{x,y,z\}}^{incident} \\
 &= \frac{4\pi a^3}{3} \varepsilon E_{\{x,y,z\}}^{incident}
 \end{aligned} \tag{36}$$

and the “contrast”  $(\hat{\varepsilon} - 1)$  in an expression for the dipole-moment indicates a “Born” result. In contrast, an expression of the form

$$\frac{(\hat{\varepsilon} - 1)}{(\hat{\varepsilon} + 2)} \tag{37}$$

indicates a “boundary value” solution of the problem of a dielectric sphere immersed in a static electric field. For example, in the case of a sphere, the field inside the sphere in a boundary value approach is

$$\begin{aligned}
 E^{inside} &= \frac{3}{(\hat{\varepsilon} + 2)} E^{incident} \\
 &\cong E^{incident}, \hat{\varepsilon} \cong 1
 \end{aligned} \tag{38}$$

Substituting the first line of equation (38) into the first line of (36) gives

$$\begin{aligned}
 p_{\{x,y,z\}} &= \varepsilon_o \int_V (\hat{\varepsilon} - 1) E^{inside} d\mathbf{r}' \\
 &= 3\varepsilon_o \int_V \frac{(\hat{\varepsilon} - 1)}{(\hat{\varepsilon} + 2)} E_{\{x,y,z\}}^{incident} d\mathbf{r}' \\
 &= 3\varepsilon_o \frac{(\hat{\varepsilon} - 1)}{(\hat{\varepsilon} + 2)} \frac{4\pi a^3}{3} E_{\{x,y,z\}}^{incident} \\
 &= 4\pi a^3 \frac{(\hat{\varepsilon} - 1)}{(\hat{\varepsilon} + 2)} \varepsilon_o E_{\{x,y,z\}}^{incident}
 \end{aligned} \tag{39}$$

Equation (39) yields the proper limit

$$\lim_{\sigma \rightarrow \infty} p_{\{x,y,z\}} = 4\pi a^3 \varepsilon_o E_{\{x,y,z\}}^{incident} \tag{40}$$

Equation (34) shows that, in general, we need to solve a boundary value problem to determine the exact values for the polarizability for

an arbitrary shaped target. Stratton (1941) solves a boundary value problem for a dielectric sphere and ellipsoid. Both solutions can be analytically continued to treat the case of a complex permittivity to include the effect of a finite conductivity. Van de Hulst (1957) also gives the electric polarizability for a conducting ellipsoid and sphere. Collin (1960) gives the electric and magnetic polarizability for perfectly conducting spheres, ellipsoids, and spheroids.

We summarize the electric and magnetic polarizability for a sphere

$$\alpha_e = 4\pi a^3 \varepsilon_o \frac{(\hat{\varepsilon} - 1)}{(\hat{\varepsilon} + 2)}$$

$$\hat{\varepsilon} = \varepsilon_r + \frac{i\sigma}{\omega \varepsilon_o}$$
(41)

and for  $\frac{\sigma}{\omega \varepsilon_o} \gg 1$ ,

$$\alpha_e = 4\pi a^3 \left( \frac{i\sigma}{\omega \varepsilon_o} \right) \varepsilon_o = \frac{4\pi a^3 \sigma}{-i\omega}$$
(42)

and the corresponding electric current-moment is

$$I dl = -i\omega \alpha_e (\equiv p) = 4\pi a^3 \sigma$$
(43)

in agreement with the Van de Hulst result in equation (34) given above. The corresponding magnetic dipole moment is

$$\alpha_m = -2\pi a^3 [3(M - iN)]$$

$$= -2\pi a^3 \begin{cases} 1, & \sigma \rightarrow \infty \\ \frac{i\omega \mu_o a^2}{15}, & \sigma \rightarrow 0 \end{cases}$$
(44)

## 4.2 Polarizability for an Ellipsoid

Stratton (pages 212-213) solved the boundary value problem for an ellipsoid in a static electric field and the result is

$$E_{\{x,y,z\}}^{perturbed} = \frac{E^{incident}}{1 + \frac{abc}{2\varepsilon_2} (\varepsilon_{object} - \varepsilon_2) L_{\{x,y,z\}}}$$
(45)



so that the electric polarizability is

$$\alpha_{\{ex,ey,ez\}} = \frac{(\varepsilon_{object} - \varepsilon_2) \left( \frac{4\pi abc}{3} \right) E^{incident}}{1 + \frac{abc}{2\varepsilon_2} L_{\{x,y,z\}}} \quad (46)$$

where

$$L_i = \frac{l_1 l_2 l_3}{2} \int_0^\infty \frac{dx}{(x + l_i^2) \sqrt{(x + l_1^2)(x + l_2^2)(x + l_3^2)}} \quad (47)$$

$$L_1 + L_2 + L_3 = 1$$

The result in (47) agrees with Ishimaru (page 291, equation (10-47)). By duality, the magnetic polarizability for an ellipsoid is

$$\alpha_m = \frac{(\mu_{object} - \mu_2) \left( \frac{4\pi abc}{3} \right) H^{incident}}{1 + \frac{abc}{2\mu_2} (\mu_{object} - \mu_2) L_i} \quad (48)$$

For a spheroid, two axes of the ellipsoid are equal ( $L_i = L_j$ ).

## 5. SCATTERED FIELDS IN REGION (1) FOR A VMD IN REGION (1)

### 5.1 Theory

The quasi-static magnetic field does not depend of the medium properties; i.e., changes in  $\varepsilon$  or  $\sigma$ , and therefore, should be the optimum source for detecting most underground objects. The induced dipole (electric and magnetic) at the target in region (2) are the product of the electric and magnetic polarizabilities and the unperturbed electric and magnetic fields. The unperturbed fields in equations (20) and (24) are evaluated at

$$\begin{aligned} \underline{R}' &= 0 \\ \underline{R} &= (x_o, y_o, -d) \end{aligned} \quad (49)$$

and from (29) and (35) the induced electric and magnetic dipole moments are

$$\begin{aligned}
 m_x &= \alpha_{mx} \cos \phi' H_{2\rho}^{unpert}(x_o, y_o, -d) \\
 m_y &= \alpha_{my} \sin \phi' H_{2\rho}^{unpert}(x_o, y_o, -d) \\
 m_z &= \alpha_{mz} H_{2z}^{unpert}(x_o, y_o, -d) \\
 p_x &= \alpha_{ex} (-\sin \phi') E_{2\phi}^{unpert}(x_o, y_o, -d) \\
 p_y &= \alpha_{ey} (\cos \phi') E_{2\phi}^{unpert}(x_o, y_o, -d) \\
 p_z &= \alpha_{ez} E_{2z}^{unpert}(x_o, y_o, -d) = 0 \text{ (TE to } z) \\
 \tan \phi' &= \frac{y_o}{x_o}
 \end{aligned} \tag{50}$$

where  $\alpha_e, \alpha_m$  depend on the particular target shape (e.g., sphere, ellipsoid, spheroid, parallelepiped). From (50) we see that the **VMD** in region 1, causes the target to reradiate a **VMD**, **HMD** and **HED**. These dipole moments are now located in region 2 (in the layer) and the field at the observation point  $\underline{R} = (x, y, z)$  corresponding to the induced moments at the secondary source point  $\underline{R} = (x, y, -d)$ , for the **VMD**, are from equations (16) and (17), modified to take into account the secondary source is in the layer, given by

$$\begin{aligned}
 H_{1x}^v(x, y, z) &= \frac{-m_z}{4\pi} \cos \phi \\
 &\quad \cdot \int_0^\infty k_\rho^2 \frac{k_{1z}}{k_{2z}} J_1 \left( k_\rho \sqrt{(x-x_o)^2 + (y-y_o)^2} \right) F_+^{TE}(z, -d) dk_\rho \\
 H_{1y}^v(x, y, z) &= \frac{-m_z}{4\pi} \sin \phi \\
 &\quad \cdot \int_0^\infty k_\rho^2 \frac{k_{1z}}{k_{2z}} J_1 \left( k_\rho \sqrt{(x-x_o)^2 + (y-y_o)^2} \right) F_+^{TE}(z, -d) dk_\rho \\
 H_{1z}^v(x, y, z) &= \frac{-im_z}{4\pi} \\
 &\quad \cdot \int_0^\infty \frac{k_\rho^3}{k_{2z}} J_0 \left( k_\rho \sqrt{(x-x_o)^2 + (y-y_o)^2} \right) F_+^{TE}(z, -d) dk_\rho
 \end{aligned}$$

$$\tan \phi = \frac{y}{x} \quad (51)$$

where the  $z$ -variation in (51) accounts for upgoing and downgoing waves, and is basically the modification of the point source variation radiating in an unbounded medium exemplified in equation (16) as

$$F(z, z') = e^{ik_z|z-z'|} \quad (52)$$

where in (51) the source is in medium 2 in figure 1, and the observer is in region 1. Implementing the boundary conditions at  $z = -d_1, z = -d_2$  Chew (1995, page 77, equation 2.4.6) obtains

$$F_+^{TE}(z, -d) = e^{ik_{1z}z} e^{ik_{1z}d_1} \tilde{T}_{21}^{TE} e^{-ik_{2z}d_1} \cdot \left[ e^{ik_{2z}d} + \tilde{R}_{23}^{TE} e^{ik_{2z}(-d+2d_2)} \right] \tilde{M}_2^{TE} \tilde{M}_1^{TE} \quad (53)$$

where, Chew gives

$$\begin{aligned} \tilde{M}_1^{TE} &= 1 \\ \tilde{M}_2^{TE} &= \left[ 1 - \tilde{R}_{23}^{TE} \tilde{R}_{21}^{TE} e^{2ik_{2z}(d_2-d_1)} \right]^{-1} \\ \tilde{R}_{23}^{TE} &= R_{23}^{TE} \\ \tilde{R}_{21}^{TE} &= -\tilde{R}_{12}^{TE} \\ \tilde{T}_{21}^{TE} &= \frac{k_{2z}}{k_{1z}} \tilde{T}_{12}^{TE} \\ \tilde{T}_{12}^{TE} &= e^{ik_{1z}d_1} S_{12} = \frac{T_{12}^{TE} e^{ik_{1z}d_1}}{1 - R_{12}^{TE} \tilde{R}_{23}^{TE} e^{2ik_{1z}(d_2-d_1)}} \cong \frac{2k_{1z} e^{ik_{1z}d_1}}{k_{1z} + k_{2z}} \end{aligned} \quad (54)$$

Using equation (22) we approximate the reflection and transmission coefficients in (54) as follows:

$$\begin{aligned} R_{12}^{TE} &= \frac{k_{1z} - k_{2z}}{k_{1z} + k_{2z}} \cong \frac{ik_\rho - ik_\rho + \frac{ik_2^2}{2k_\rho}}{2ik_\rho} = \frac{k_2^2}{4k_\rho^2} \\ R_{23}^{TE} &= \frac{k_{2z} - k_{3z}}{k_{2z} + k_{3z}} \cong \frac{ik_\rho - \frac{ik_2^2}{2k_\rho} - ik_\rho + \frac{ik_3^2}{2k_\rho}}{2ik_\rho} = -\frac{(k_2^2 - k_3^2)}{4k_\rho^2} \end{aligned}$$

$$\begin{aligned}
T_{12}^{TE} &= \frac{2k_{1z}}{k_{1z} + k_{2z}} \cong \frac{2ik_\rho}{2ik_\rho - \frac{k_2^2}{2k_\rho}} = \frac{1}{1 - \frac{k_2^2}{4k_\rho^2}} \cong 1 + \frac{k_2^2}{4k_\rho^2} \\
T_{21}^{TE} &= \frac{k_{2z}}{k_{1z}} T_{12}^{TE} \cong \left( \frac{ik_\rho - \frac{ik_2^2}{2k_\rho}}{ik_\rho} \right) \left( 1 + \frac{k_2^2}{4k_\rho^2} \right) \cong 1 - \frac{k_2^2}{4k_\rho^2} \\
T_{12}^{TE} R_{23}^{TE} T_{21}^{TE} &\cong - \left( 1 + \frac{k_2^2}{4k_\rho^2} \right) \left( \frac{k_2^2 - k_3^2}{4k_\rho^2} \right) \left( 1 - \frac{k_2^2}{4k_\rho^2} \right) \cong - \frac{(k_2^2 - k_3^2)}{4k_\rho^2} \\
e^{2ik_{2z}(d_2-d_1)} &\cong e^{-k_\rho(d_2-d_1)} \\
A_2^{TE} &\cong T_{12}^{TE} \\
\tilde{R}_{12}^{TE} &\cong \frac{k_2^2}{4k_\rho^2} - \frac{(k_2^2 - k_3^2)}{4k_\rho^2} e^{-2k_\rho(d_2-d_1)} \tag{55}
\end{aligned}$$

Substituting the approximations (54) and (55) in to (53) gives the approximate result

$$\begin{aligned}
F_+^{TE}(z, -d) &\cong \frac{2k_{1z}}{k_{1z} + k_{2z}} e^{ik_{1z}(z+d_1)} e^{-ik_{2z}d} \\
&\quad \cdot \left[ e^{ik_{2z}d} - \frac{(k_2^2 - k_3^2)}{4k_\rho^2} e^{ik_{2z}(-d+2d_2)} \right] \tag{56} \\
&\cong e^{-k_\rho(z+d)} - \frac{(k_2^2 - k_3^2)}{4k_\rho^2} e^{ik_{2z}(z-d+2d_2)}
\end{aligned}$$

where the two exponentials in (56) can be interpreted as a secondary sources located as shown in figure 2.

We now consider the reradiated fields from the **HMD**. Again, from equations (1), (2) and (3) with the dipole pointing in the  $\rho'$ -direction, and given by

$$\begin{aligned}
\pi_x^m &= \frac{im_x}{4\pi} \int_0^\infty \frac{k_\rho}{k_z} J_o(k_\rho|\underline{\rho} - \underline{\rho}'|) e^{ik_z|z-z'|} dk_\rho \tag{57} \\
\pi_x^m &\rightarrow -i\omega\mu_o m_x \pi_x^m
\end{aligned}$$

Substituting (57) into the third equation in (1) gives

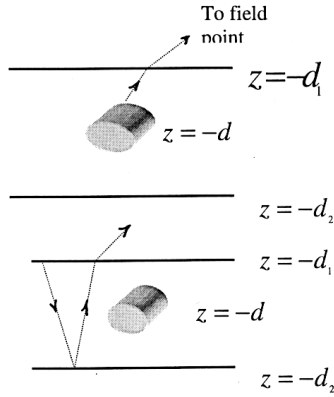


**Figure 2.** Geometrical interpretation of the Green's Function,  $F_+(z, -d)$  for a source in the layered medium.

$$\begin{aligned}
 H_{1z}^h(\rho, z) &= \frac{e_z}{i\omega\mu} \frac{\partial^2 \pi_x^m}{\partial x \partial z} \\
 &= \left( \frac{-m_x}{4\pi} \right) \cos \phi' \int_0^\infty k_\rho^2 J_1(k_\rho |\underline{\rho} - \underline{\rho}'|) e^{ik_z |z - z'|} dk_\rho \\
 \cos \phi' &= \frac{x'}{\sqrt{x'^2 + y'^2}} \tag{58}
 \end{aligned}$$

As in (51) we are considering the case where the target is reradiating, and the exponential factor  $e^{ik_{1z}|z-z'|}$  needs to be replaced by  $F_+^{TE}(z, -d)$  for a “secondary source” in region 2 radiating to an observer in region 1.

The transverse components of the magnetic field for a **HMD** are obtained by substituting (58) into (15) yielding

$$\begin{aligned}
 \underline{H}_{1t}^h(\rho, z) &= \frac{1}{k_\rho^2 e_\rho} \frac{\partial^2 H_{1z}^{unpert}}{\partial \rho \partial z} \\
 \frac{\partial J_1}{\partial \rho} &= k_\rho \left[ J_0(k_\rho |\underline{\rho} - \underline{\rho}'|) - \frac{J_1(k_\rho |\underline{\rho} - \underline{\rho}'|)}{k_\rho |\underline{\rho} - \underline{\rho}'|} \right]
 \end{aligned}$$

$$H_{\{1x,1y\}}^h = \left( \frac{-im_x \cos \phi'}{4\pi} \right) \left( \frac{\cos \phi}{\sin \phi} \right) \cdot \int_0^\infty k_{1z} k_\rho^2 \left[ J_0(k_\rho |\underline{\rho} - \underline{\rho}'|) - \frac{J_1(k_\rho |\underline{\rho} - \underline{\rho}'|)}{k_\rho |\underline{\rho} - \underline{\rho}'|} \right] e^{ik_{1z}|z-z'|} dk_\rho \quad (59)$$

The next case of reradiation (scatter) by the target comes from the induced **HED** (horizontal electric dipole). This dipole is also pointing in the  $\rho'$ -direction, and the Hertz potential is given by

$$\pi_x^e = \left( \frac{i}{4\pi} \right) (-i\omega p_x) \int_0^\infty \frac{k_\rho}{k_z} J_0(k_\rho |\underline{\rho} - \underline{\rho}'|) e^{ik_z|z-z'|} dk_\rho \quad (60)$$

Substituting (59) into the second equation in (1) gives

$$\begin{aligned} \underline{H}_{1z}^h(\rho, z) &= -\underline{e}_z \frac{\partial \pi_x^e}{\partial y} \\ &= \underline{e}_z \left( \frac{-ip_x}{4\pi} \right) \int_0^\infty \frac{k_\rho}{k_{1z}} J_0(k_\rho |\underline{\rho} - \underline{\rho}'|) e^{ik_{1z}|z'-z|} dk_\rho \\ &= \underline{e}_z \left( \frac{ip_x \sin \phi'}{4\pi} \right) \int_0^\infty \frac{k_\rho^2}{k_{1z}} J_1(k_\rho |\underline{\rho} - \underline{\rho}'|) e^{ik_{1z}|z-z'|} dk_\rho \quad (61) \end{aligned}$$

The transverse components of the magnetic field for a **HED** are obtained by substituting (61) into (15) giving

$$\begin{aligned} H_{\{1x,1y\}}^e(\rho, z) &= \frac{p_x \sin \phi'}{4\pi} \left( \frac{\cos \phi}{\sin \phi} \right) \\ &\cdot \int_0^\infty k_\rho \left[ J_0(k_\rho |\underline{\rho} - \underline{\rho}'|) - \frac{J_1(k_\rho |\underline{\rho} - \underline{\rho}'|)}{k_\rho |\underline{\rho} - \underline{\rho}'|} \right] e^{ik_{1z}|z-z'|} dk_\rho \quad (62) \end{aligned}$$

The total scattered magnetic field in region 1 from the scatter from a buried object in region 2, in equation (25) is from equations (51), (59)

and (62), for the  $x$ -,  $y$ - components:

$$\begin{aligned}
H_{\{1x,1y\}}^S(\rho, z) &= \left( \frac{-m_z}{4\pi} \right) \begin{pmatrix} \cos \phi \\ \sin \phi \end{pmatrix} \\
&\cdot \int_0^\infty \frac{k_{1z} k_\rho^2}{k_{2z}} J_1(k_\rho |\underline{\rho} - \underline{\rho}'|) F_+^{TE}(z, -d) dk_\rho \\
&+ \left( \frac{-m_x \cos \phi'}{4\pi} \right) \begin{pmatrix} \cos \phi \\ \sin \phi \end{pmatrix} \\
&\cdot \int_0^\infty k_{1z} k_\rho \left[ J_0(k_\rho |\underline{\rho} - \underline{\rho}'|) - \frac{J_1(k_\rho |\underline{\rho} - \underline{\rho}'|)}{k_\rho |\underline{\rho} - \underline{\rho}'|} \right] F_+^{TE}(z, -d) dk_\rho \\
&+ \left( \frac{p_x \sin \phi'}{4\pi} \right) \begin{pmatrix} \cos \phi \\ \sin \phi \end{pmatrix} \\
&\cdot \int_0^\infty k_\rho \left[ J_0(k_\rho |\underline{\rho} - \underline{\rho}'|) - \frac{J_1(k_\rho |\underline{\rho} - \underline{\rho}'|)}{k_\rho |\underline{\rho} - \underline{\rho}'|} \right] F_+^{TE}(z, -d) dk_\rho
\end{aligned} \tag{63}$$

For the  $z$ -component:

$$\begin{aligned}
H_{1z}^S(\rho, z) &= \left( \frac{-im_z}{4\pi} \right) \int_0^\infty \frac{k_\rho^3}{k_{1z}} J_1(k_\rho |\underline{\rho} - \underline{\rho}'|) F_+^{TE}(z, -d) dk_\rho \\
&+ \left( \frac{-m_x \cos \phi'}{4\pi} \right) \int_0^\infty k_\rho^2 J_1(k_\rho |\underline{\rho} - \underline{\rho}'|) F_+^{TE}(z, -d) dk_\rho \\
&+ \left( \frac{ip_x \sin \phi'}{4\pi} \right) \int_0^\infty \frac{k_\rho^2}{k_{2z}} J_1(k_\rho |\underline{\rho} - \underline{\rho}'|) F_+^{TE}(z, -d) dk_\rho
\end{aligned} \tag{64}$$

The total magnetic field in region 1 for the case of a **VMD** source is

$$H_{\{1x,1y,1z\}}^{total} = H_{1z}^{incident} + H_{\{1x,1y,1z\}}^S \tag{65}$$

where, from equations (14) and (55) the incident fields is

$$H_{1z}^{incident}(\rho, z) = \left( \frac{-im}{4\pi} \right) \int_0^{\infty} \frac{k_{\rho}^3}{k_{1z}} J_0(k_{\rho}\rho) \cdot \left\{ e^{-k_{\rho}|z|} + \tilde{R}_{12}^{TE} e^{ik_{1z}z + 2ik_{1z}d_1} \right\} dk_{\rho} \quad (66)$$

We complete this section by examining in detail the  $z$ -component of the total field. The remaining terms are the magnetic polarizability,  $m_{x,y,z}$ . From equation (50) we see this involves the unperturbed field  $H_{2z}^{unpert}(x_o, y_o, -d)$  incident on the object. From equation (20) and the approximations in (55) this is given by

$$m_z = \alpha_{mz} H_{2z}^{unpert}(\rho_o, -d) = \alpha_{mz} \left( \frac{-im}{4\pi} \right) \int_0^{\infty} \frac{k_{\rho}^3}{k_{1z}} J_0(k_{\rho}\sqrt{x_o^2 + y_o^2}) \cdot A_2^{TE} \left[ e^{ik_{2z}d} + R_{23}^{TE} e^{2ik_{2z}d_2 - ik_{2z}d} \right] dk_{\rho} \quad (67)$$

and,

$$m_{\{x,y\}} = \left( \frac{im}{4\pi} \right) \begin{pmatrix} \alpha_{mx} \cos \phi \\ \alpha_{my} \sin \phi \end{pmatrix} \int_0^{\infty} k_{\rho}^2 J_1(k_{\rho}\sqrt{x_o^2 + y_o^2}) \cdot A_2^{TE} [e^{ik_{2z}d} + R_{23}^{TE} e^{2ik_{2z}d_2 - ik_{2z}d}] dk_{\rho} \quad (68)$$

From equation (50), we also need to compute the electric dipole moments for the VMD source. These involve the unperturbed electric fields at the target. From equation (24) we have

$$p_{\{x,y\}} = \left( \frac{\omega\mu_o m}{4\pi} \right) \begin{pmatrix} -\alpha_{ex} \sin \phi' \\ \alpha_{ey} \cos \phi' \end{pmatrix} \int_0^{\infty} \frac{k_{\rho}^2}{k_{1z}} J_1(k_{\rho}\sqrt{x_o^2 + y_o^2}) \cdot A_2^{TE} [e^{ik_{2z}d} + R_{23}^{TE} e^{2ik_{2z}d_2 - ik_{2z}d}] dk_{\rho} \quad (69)$$

$$p_z = 0 \quad (\text{TE to } z)$$

where,  $\omega\mu_o m$  comes from the  $\phi$ -component of the unperturbed electric field. The total  $z$ -component of the magnetic field at the observer



is

$$\begin{aligned}
 H_{1z}^{total}(x, y, z) = & \left( \frac{-im_z}{4\pi} \right) \\
 & \cdot \int_0^\infty \frac{k_\rho^3}{k_{1z}} J_0 \left( k_\rho \sqrt{(x-x_o)^2 + (y-y_o)^2} \right) F_+^{TE}(z, -d) dk_\rho \\
 & + \left( \frac{-m_x \cos \phi'}{4\pi} \right) \\
 & \cdot \int_0^\infty k_\rho^2 J_1 \left( k_\rho \sqrt{(x-x_o)^2 + (y-y_o)^2} \right) F_+^{TE}(z, -d) dk_\rho \\
 & + \left( \frac{ip_x \sin \phi'}{4\pi} \right) \\
 & \cdot \int_0^\infty \frac{k_\rho^2}{k_{2z}} J_1 \left( k_\rho \sqrt{(x-x_o)^2 + (y-y_o)^2} \right) F_+^{TE}(z, -d) dk_\rho \\
 & + \left( \frac{-im}{4\pi} \right) \int_0^\infty \frac{k_\rho^3}{k_{1z}} J_0(k_\rho \sqrt{x^2 + y^2}) \\
 & \cdot \left[ e^{ik_{1z}|z|} + \tilde{R}_{12}^{TE} e^{ik_{1z}z + 2ik_{1z}d_1} \right] dk_\rho \tag{70}
 \end{aligned}$$

and we write (70) by defining the following integrals,

$$\begin{aligned}
 H_{1z}^{total}(x, y, z) = & \left( \frac{-im}{4\pi} \right) I_1 \\
 & + \left( \frac{-m_x \cos \phi'}{4\pi} \right) I_2 \\
 & + \left( \frac{ip_x \sin \phi'}{4\pi} \right) I_3 \\
 & + \left( \frac{-im}{4\pi} \right) I_4 \tag{71}
 \end{aligned}$$

together with the integrals for the magnetic and electric polarizability

$$\begin{aligned}
 m_x &= \left(\frac{im}{4\pi}\right) \begin{pmatrix} \alpha_{mx} \cos \phi \\ \alpha_{my} \sin \phi \end{pmatrix} I_5 \\
 & \quad y \\
 m_z &= \left(\frac{im}{4\pi}\right) \alpha_{mz} I_6 \\
 p_x &= \left(\frac{\omega\mu_o m}{4\pi}\right) \begin{pmatrix} -\alpha_{ex} \cos \phi' \\ \alpha_{ey} \sin \phi' \end{pmatrix} I_7 \\
 & \quad y \\
 p_z &= 0
 \end{aligned} \tag{72}$$

These integrals are defined by

$$\begin{aligned}
 I_1 &= \int_0^\infty \frac{k_\rho^3}{k_{2z}} J_o \left( k_\rho \sqrt{(x-x_o)^2 + (y-y_o)^2} \right) F_+^{TE}(z, -d) dk_\rho \\
 I_2 &= \int_0^\infty k_\rho^2 J_1 \left( k_\rho \sqrt{(x-x_o)^2 + (y-y_o)^2} \right) F_+^{TE}(z, -d) dk_\rho \\
 I_3 &= \int_0^\infty \frac{k_\rho^2}{k_{2z}} J_1 \left( k_\rho \sqrt{(x-x_o)^2 + (y-y_o)^2} \right) F_+^{TE}(z, -d) dk_\rho \\
 I_4 &= \int_0^\infty \frac{k_\rho^3}{k_{1z}} J_o(k_\rho \sqrt{x^2 + y^2}) \left[ e^{ik_{1z}|z|} + \tilde{R}_{12}^{TE} e^{ik_{1z}z + 2ik_{1z}d_1} \right] dk_\rho \\
 I_5 &= \int_0^\infty k_\rho^2 J_1(k_\rho \sqrt{x^2 + y^2}) A_2^{TE} \left[ e^{ik_{1z}d} + R_{23}^{TE} e^{2ik_{2z}d_2 - ik_{2z}d} \right] dk_\rho \\
 I_6 &= \int_0^\infty \frac{k_\rho^3}{k_{1z}} J_o(k_\rho \sqrt{x^2 + y^2}) A_2^{TE} \left[ e^{ik_{1z}d} + R_{23}^{TE} e^{2ik_{2z}d_2 - ik_{2z}d} \right] dk_\rho \\
 I_7 &= \int_0^\infty \frac{k_\rho^2}{k_{1z}} J_1(k_\rho \sqrt{x^2 + y^2}) A_2^{TE} \left[ e^{ik_{1z}d} + R_{23}^{TE} e^{2ik_{2z}d_2 - ik_{2z}d} \right] dk_\rho \tag{73}
 \end{aligned}$$

In the quasi-static regime, the integrals in (73) can be approximated

as (Gröbner and Hofreiter, 1965)

$$\begin{aligned}
 I_1 &\cong -i \int_0^{\infty} k_{\rho}^2 J_0 \left( k_{\rho} \sqrt{(x-x_o)^2 + (y-y_o)^2} \right) \\
 &\quad \cdot \left[ e^{-k_{\rho}(z+d)} - \frac{(k_2^2 - k_3^2)}{4k_{\rho}^2} e^{-k_{\rho}(z-d+2d_2)} \right] dk_{\rho} \\
 &= -i \left\{ \frac{\left[ \frac{2(z+d)^2 - (x-x_o)^2 - (y-y_o)^2}{[(x-x_o)^2 + (y-y_o)^2 + (z+d)^2]^{\frac{3}{2}}} \right]}{-\frac{(k_2^2 - k_3^2)}{4\sqrt{(x-x_o)^2 + (y-y_o)^2 + (z-d+2d_2)^2}}} \right\} \quad (74)
 \end{aligned}$$

$$\begin{aligned}
 I_2 &\cong \int_0^{\infty} k_{\rho}^2 J_1 \left( k_{\rho} \sqrt{(x-x_o)^2 + (y-y_o)^2} \right) \\
 &\quad \cdot \left[ e^{-k_{\rho}(z+d)} - \frac{(k_2^2 - k_3^2)}{4k_{\rho}^2} e^{-k_{\rho}(z-d+2d_1)} \right] dk_{\rho} \\
 &= \left\{ \frac{\left[ \frac{3(z+d)\sqrt{(x-x_o)^2 + (y-y_o)^2}}{[(x-x_o)^2 + (y-y_o)^2 + (z+d)^2]^{\frac{3}{2}}} \right]}{-\frac{(k_2^2 - k_3^2) \left[ \sqrt{(x-x_o)^2 + (y-y_o)^2 + (z-d+2d_1)^2} - (z-d+2d_1) \right]}{\sqrt{(x-x_o)^2 + (y-y_o)^2} \sqrt{(x-x_o)^2 + (y-y_o)^2 + (z-d+2d_1)^2}}} \right\} \quad (75)
 \end{aligned}$$

$$\begin{aligned}
 I_3 &\cong -i \int_0^{\infty} k_{\rho} J_1 \left( k_{\rho} \sqrt{(x-x_o)^2 + (y-y_o)^2} \right) \\
 &\quad \cdot \left[ e^{-k_{\rho}(z+d)} - \frac{(k_2^2 - k_3^2)}{4k_{\rho}^2} e^{-k_{\rho}(z-d+2d_1)} \right] dk_{\rho} \\
 &= -i \left\{ \frac{\left[ \frac{\sqrt{(x-x_o)^2 + (y-y_o)^2}}{[(x-x_o)^2 + (y-y_o)^2 + (z+d)^2]^{\frac{3}{2}}} \right]}{-\frac{(k_2^2 - k_3^2) \left[ \sqrt{(x-x_o)^2 + (y-y_o)^2 + (z-d+2d_1)^2} - (z-d+2d_1) \right]}{4\sqrt{(x-x_o)^2 + (y-y_o)^2}}} \right\} \quad (76)
 \end{aligned}$$

$$\begin{aligned}
I_4 &\cong -i \int_0^\infty k_\rho^2 J_0(k_\rho \sqrt{x^2 + y^2}) \\
&\quad \cdot \left[ e^{-k_\rho |z|} + \left( \frac{k_2^2}{4k_\rho^2} - \frac{(k_2^2 - k_3^2)}{4k_\rho^2} e^{-2k_\rho(d_2 - d_1)} \right) e^{-k_\rho z - 2k_\rho d_1} \right] dk_\rho \\
&= -i \left\{ \begin{aligned} &\frac{\left[ \frac{2z^2 - x^2 - y^2}{x^2 + y^2 + z^2} \right]^{\frac{3}{2}}}{k_2^2} \\ &+ \frac{k_2^2}{4\sqrt{x^2 + y^2 + (z + 2d_1)^2}} \\ &- \frac{(k_2^2 - k_3^2)}{4\sqrt{x^2 + y^2 + (z + 2d_2)^2}} \end{aligned} \right\} \tag{77}
\end{aligned}$$

$$\begin{aligned}
I_5 &\cong \int_0^\infty k_\rho^2 J_1(k_\rho \sqrt{x^2 + y^2}) \\
&\quad \cdot \left[ e^{-k_\rho |z|} - \frac{(k_2^2 - k_3^2)}{4k_\rho^2} e^{-2k_\rho d_2 + k_\rho d} \right] dk_\rho \\
&= -i \left\{ \begin{aligned} &\frac{3d\sqrt{x_o^2 + y_o^2}}{\left[ x_o^2 + y_o^2 + d^2 \right]^{\frac{3}{2}}} \\ &- \frac{(k_2^2 - k_3^2) \left[ \sqrt{x_o^2 + y_o^2 + (2d_2 - d)^2} - (2d_2 - d) \right]}{\sqrt{x_o^2 + y_o^2} \sqrt{x_o^2 + y_o^2 + (2d_2 - d)^2}} \end{aligned} \right\} \tag{78}
\end{aligned}$$

$$\begin{aligned}
I_6 &\cong -i \int_0^\infty k_\rho^2 J_0(k_\rho \sqrt{x^2 + y^2}) \\
&\quad \cdot \left[ e^{-k_\rho |z|} - \frac{(k_2^2 - k_3^2)}{4k_\rho^2} e^{-k_\rho(2d_2 - d)} \right] dk_\rho \\
&= -i \left\{ \begin{aligned} &\frac{2d^2 - x_o^2 - y_o^2}{\left[ x_o^2 + y_o^2 + d^2 \right]^{\frac{3}{2}}} \\ &- \frac{(k_2^2 - k_3^2)}{4\sqrt{x_o^2 + y_o^2 + (2d_2 - d)^2}} \end{aligned} \right\} \tag{79}
\end{aligned}$$

$$\begin{aligned}
 I_7 &\cong -i \int_0^{\infty} k_{\rho} J_1(k_{\rho} \sqrt{x^2 + y^2}) \\
 &\quad \cdot \left[ e^{-k_{\rho} d} - \frac{(k_2^2 - k_3^2)}{4k_{\rho}^2} e^{-2k_{\rho} d_2 + k_{\rho} d} \right] dk_{\rho} \\
 &= -i \left\{ \frac{\sqrt{x_o^2 + y_o^2}}{\left[ x_o^2 + y_o^2 + d^2 \right]^{\frac{3}{2}}} \right. \\
 &\quad \left. - \frac{(k_2^2 - k_3^2) \left[ \sqrt{x_o^2 + y_o^2 + d^2} - 2d_2 \right]}{4\sqrt{x_o^2 + y_o^2}} \right\} \quad (80)
 \end{aligned}$$

## 5.2 Example 1:

For the first example, we show the field scattered by an oblate spheroid. This example was chosen because published data exists for this example and therefore serves as a comparison for the results presented in this work (Hill and Cavcey, 1987). The parameter values for this example are given in Table I Since the incident field is much larger than the scattered field, in all examples only the scattered field is shown.

The magnetic polarizability for this example is

$$\begin{aligned}
 \alpha_{mz} &= \frac{-2V}{1 + L} \\
 V &= \frac{4\pi}{3} ab^2 \\
 L &= \frac{b^2}{2a^2 e^3} \left( \ln \frac{1+e}{1-e} - 2e \right) \\
 e &= \sqrt{1 - \left( \frac{b}{a} \right)^2} \quad (81)
 \end{aligned}$$

Figure 3 shows a plot of the field scattered by the buried oblate spheroid versus lateral distance. Both the results using equation (64) and results from Hill and Cavcey (1987) are show for comparison.

Parameter	Value
frequency	3 KHz
$\lambda_o$	100 Km
$\varepsilon_1 = \varepsilon_o$	
$\sigma_1$	0
$k_1^2 = \omega^2 \mu_o \varepsilon_o$	$\left(\frac{2\pi}{\lambda_o}\right)^2 \cong 3.9478 \times 10^{-9}$
$\varepsilon_2 = \varepsilon_o$	
$\sigma_2$ (sea floor)	0
$\lambda = \lambda_o$	
$k_2^2 = k_1^2$	
$k_3^2 = k_1^2$	
$\sigma_s$ (scatterer)	Perfect conductor
$\mu_s = \mu_o$	$4\pi \times 10^{-7}$ H/m
Spheroid semi-major axis	0.15 m
Spheroid semi-minor axis	0.05 m
$d_1$ transmitter height above sea	0.25 m
$d_2$ sea floor depth below transmitter	1. m
d scatterer depth	0.25m

**Table I.** Parameter Values for an Oblate spheroid in Free Space

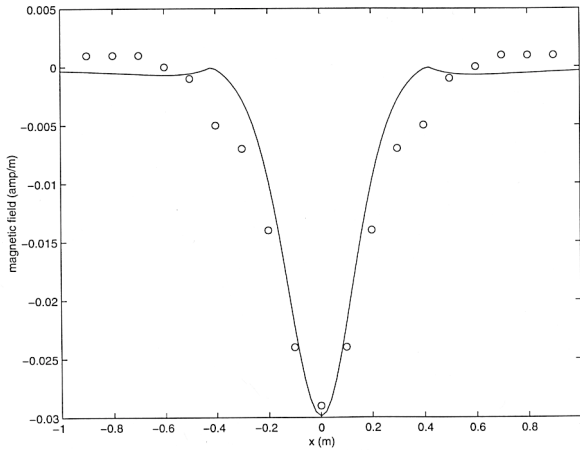


**Figure 3.** Contour plot of  $|H_{1z}^S(x)|$  for the parameter values in Table I. Open circles are Hill and Cavcey (1987) and solid line used equation (64).

Parameter	Value
frequency	3 KHz
$\lambda_o$	100 Km
$\varepsilon_1$	81
$\sigma_1$	4 Mho/m
$k_1^2 = \omega^2 \mu_o \varepsilon_o$	$\left(\frac{2\pi}{\lambda_o}\right)^2 \cong 3.9478 \times 10^{-9}$
$\varepsilon_2$ (sea floor)	20
$\sigma_2$ (sea floor)	0.4 Mho/m
$\lambda = \frac{\lambda_o}{4899}$	20.4 m
$k_2^2 = k_1^2 \left( \varepsilon_{r1} + i \frac{\sigma_1}{\omega \varepsilon_o} \right)$	$\cong i 0.09478$
$k_3^2 = k_1^2 \left( \varepsilon_{r2} + i \frac{\sigma_2}{\omega \varepsilon_o} \right)$	$\cong i 0.009478$
$\sigma_s$ (scatterer)	Perfect conductor
$\mu_s = \mu_o$	$4\pi \times 10^{-7}$ H/m
$d_1$ transmitter height above sea	1 m
$a$ (sphere radius)	4 m
$d_2$ (sea floor depth)	11 m
$d$ (scatterer depth)	6 m

**Table II.** Parameter Values for an Sphere Sea Water

**Example 2:**

This example is a conducting sphere in sea water. The parameter values for this example are given in Table II.

The parameter values and geometry yield the following results for the induced electric and magnetic dipole moments in equation (50).

$$\begin{aligned}
 m_x &= \alpha_{mx} H_{2\rho}^{unpert}(0, 0, -d) \\
 m_y &= 0 \\
 m_z &= \alpha_{mz} H_{2\rho}^{unpert}(0, 0, -d) \\
 p_x &= 0 \\
 p_y &= \alpha_{ey} E_{2\phi}^{unpert}(0, 0, -d) \\
 p_z &= 0
 \end{aligned} \tag{82}$$

From equation (64) the  $z$ -component of the scattered field is

$$\begin{aligned}
 H_{1z}^S(x, y, z) &= \left( \frac{-im_z}{4\pi} \right) \int_0^\infty \frac{k_\rho^3}{k_{1z}} J_0(k_\rho \sqrt{x^2 + y^2}) F_+^{TE}(z, -d) dk_\rho \\
 &+ \left( \frac{-m_x}{4\pi} \right) \int_0^\infty k_\rho^2 J_1(k_\rho \sqrt{x^2 + y^2}) F_+^{TE}(z, -d) dk_\rho
 \end{aligned} \tag{83}$$

The second integral in (83) is zero because

$$\begin{aligned}
 m_x &= \left( \frac{im\alpha_{mx}}{4\pi} \right) \int_0^\infty k_\rho^2 J_1(k_\rho \cdot 0) A_2^{TE} \left[ e^{ik_{2z}d} + R_{23}^{TE} e^{2ik_{2z}d_2 - ik_{2z}d} \right] dk_\rho \\
 &= 0 \\
 m_z &= \left( \frac{im\alpha_{mz}}{4\pi} \right) \int_0^\infty \frac{k_\rho^3}{k_{2z}} A_2^{TE} \left[ e^{ik_{2z}d} + R_{23}^{TE} e^{2ik_{2z}d_2 - ik_{2z}d} \right] dk_\rho
 \end{aligned} \tag{84}$$

The third integral of (83) is zero for the same reason in (84); i.e., the argument of the Bessel function of order one of the first kind is zero. However, in general the contribution to the scattered magnetic field from the induced electric dipole moment is of order  $k$  times the scattered electric field as shown below.

$$\begin{aligned}
 p_{\{x,y\}} &= \left( \frac{\omega\mu_o m}{4\pi} \right) \begin{pmatrix} -\alpha_{ex} \\ \alpha_{ey} \end{pmatrix} \int_0^\infty \dots dk_\rho \\
 H_{1z}^S &= \left( \frac{\omega p_y}{4\pi} \right) \cos \phi' \int_0^\infty \dots dk_\rho \\
 &= \left( \frac{\omega^2 \mu_o m}{(4\pi)^2} \right) \cos \phi' \begin{pmatrix} -\alpha_{ex} \\ \alpha_{ey} \end{pmatrix} \int_0^\infty \dots dk_\rho \int_0^\infty \dots dk_\rho \\
 &= \left( \frac{\omega^2 \mu_o \varepsilon_o m}{16\pi^2} \right) \cos \phi' \begin{pmatrix} -g_x \\ g_y \end{pmatrix} \int_0^\infty \dots dk_\rho \int_0^\infty \dots dk_\rho
 \end{aligned} \tag{85}$$



One  $k$  comes from the unperturbed induced electric field at the target, and the other  $k$  from the scattered magnetic field of a Hertzian dipole as shown in section 3.

The incident field is given in (66) and the total magnetic field is

$$\begin{aligned}
 H_{1z}^{total}(\rho, z) &= \left(\frac{-im}{4\pi}\right)I_4 + \left(\frac{-i}{4\pi}\right)I_6\left(\frac{-im\alpha_{mz}}{4\pi}\right)I_1 \\
 \alpha_{mz} &= -2\pi a^3
 \end{aligned} \tag{86}$$

Figure 4 shows a contour plot of the magnitude of the following ratio for the parameter values in Table II,

$$\begin{aligned}
 \text{ratio}(\rho, z) &= \frac{H_{1z}^{pert}(\rho, z)}{H_{1z}^{unpert}(\rho, z) + H_{1z}^{pert}(\rho, z)} \\
 &= \frac{\left(\frac{i}{4\pi}\right)\alpha_{mz}I_1I_6}{I_4 + \left(\frac{i}{4\pi}\right)\alpha_{mz}I_1I_6}
 \end{aligned} \tag{87}$$

where from equations (29), (30) and (33) the magnetic polarizability is given by

$$\alpha_{mz} = -2\pi a^3 \left( i\omega\mu_o\sigma_1 \frac{a^2}{15} \right) \tag{88}$$

From figure 4 the good agreement between the results corresponding to the exact integration of the Sommerfeld integrals (solid line in figure 4) and the quasi-static approximations (dashed line in figure 4) provides the following observations: 1) The correctness of the mathematical derivations for the quasi-static results. 2) The adequate validity of using the quasi-static results for detecting buried objects. 3) The correctness of the algorithm used to evaluate the Sommerfeld integrals. The infinite upper limit was replaced by a finite limit, and the convergence of the integrals was investigated versus the upper limit. 4) A Gaussian quadrature algorithm was used to evaluate the integrals. 4) Both results have a relative minimum along the line

$$z = \pm \frac{|\rho|}{\sqrt{2}} \tag{89}$$

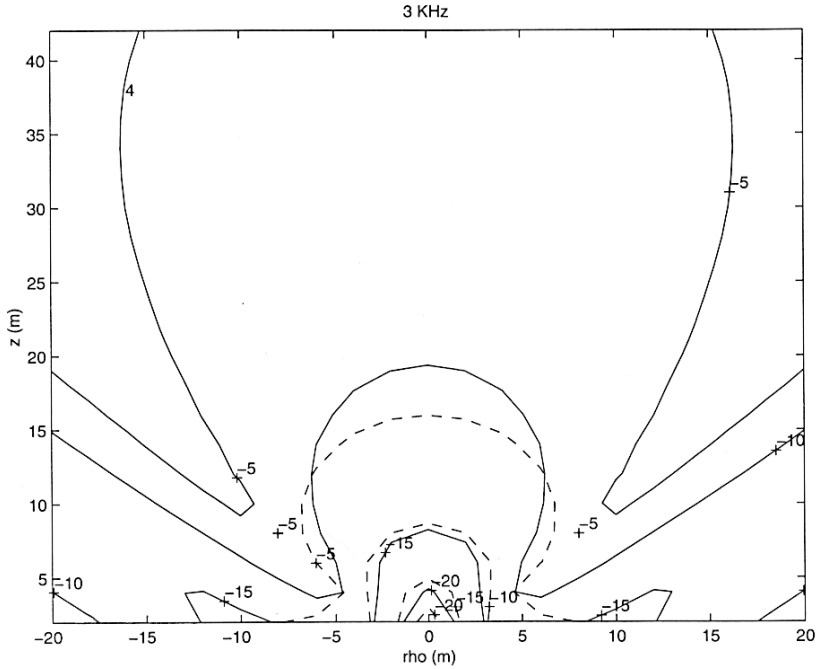


**Figure 4.** Contour plot of equation (87) for the parameter values given in Table II. ( $a = 0.15\lambda$ )

Parameter	Value
frequency	3 KHz
$\varepsilon_1$	10
$\sigma_1$	0.01 Mho/m
$\varepsilon_2$	20
$\sigma_2$	0.02 Mho/m
$\sigma_{sphere} \gg \sigma_1$	
Sphere radius	25 m
$d_1$	1 m
$d_2$	100 m
$d$	50 m

**Table III.** Parameter values for a conducting sphere in good ground

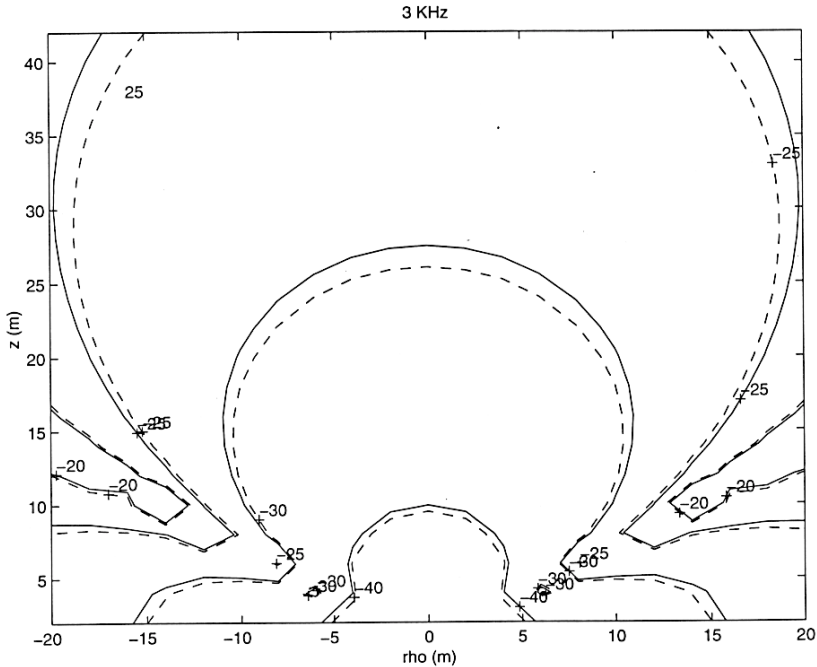


**Figure 5.** Contour plot of the magnitude of the ratio in equation (87) for the parameter values in Table III.

### Example 3:

This example is for a conducting sphere located in a layer of “good ground” (with magnetic polarizability given in equation (33)).

Figure 5 shows a contour plot of the magnitude of the ratio in equation (87) versus  $\rho, z$  for the parameter values in table III.

### Example 4:

This example is a dielectric sphere of low contrast with the dielectric constant of region 2 with parameter values given in Table IV. The total magnetic field for this case is

$$H_{1z}^{total}(x, z) = \left( \frac{-im}{4\pi} \right) \left[ I_4 + \frac{k^2(\alpha_{ey}/\epsilon_o)}{4\pi} I_3 I_7 \right]$$

$$\frac{\alpha_{ey}}{\epsilon_o} = a^3 \frac{(\hat{\epsilon} - 1)}{(\hat{\epsilon} + 2)} \quad (90)$$

Parameter	Value
frequency	10 KHz
$\varepsilon_1$	10
$\sigma_1$	0.001 Mho/m
$\varepsilon_2$	20
$\sigma_2$	0.02 Mho/m
$\varepsilon_{sphere}$	5
Sphere radius	40 m
$d_1$	1 m
$d_2$	100 m
$d$	50 m

**Table IV.** Parameter values for a dielectric sphere in sandy soil

Figure 6 shows a contour plot of the magnitude of the  $z$ -component of the total magnetic field versus  $x, z$  for the parameter values in Table IV.

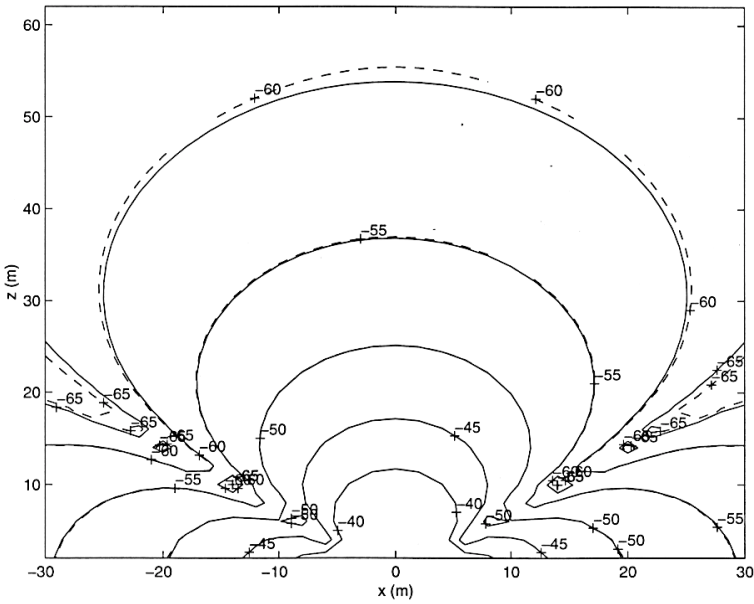


**Figure 6.** Contour plot of  $|H_{1z}^{total}(x, z)|$  for the parameter values in Table IV.

Note in figure 6 a relative maxima along the line

$$z = \pm \frac{|\rho|}{\sqrt{2}} \quad (91)$$

## 6. SCATTERED FIELDS IN REGION (1) FOR A HORIZONTAL MAGNETIC DIPOLE (HMD) IN REGION (1)

### 6.1 Theory

For the HMD case, by superposition, the scattered magnetic fields can be written in terms of rectangular components in a form similar to equation(25) as

$$\begin{aligned} H_x^S &= H_x^{m_x} + H_x^{m_y} + H_x^{m_z} + H_x^{p_x} + H_x^{p_y} + H_x^{p_z} \\ H_y^S &= H_y^{m_x} + H_y^{m_y} + H_y^{m_z} + H_y^{p_x} + H_y^{p_y} + H_y^{p_z} \\ H_z^S &= H_z^{m_x} + H_z^{m_y} + H_z^{m_z} + H_z^{p_x} + H_z^{p_y} + H_z^{p_z} \end{aligned} \quad (92)$$

where  $\underline{H}^{m_{x,y,z}}$  is the radiated field from the induced magnetic dipole moments and  $\underline{H}^{p_{x,y,z}}$  is the radiated field from the induced electric dipole moments.

Starting with the Hertz potential for a **HMD** in the  $\rho$ -direction as

$$\pi_x^m = \frac{im_x}{4\pi} \int_0^\infty \frac{k_\rho}{k_z} J_0(k_\rho |\underline{\rho} - \underline{\rho}'|) e^{ik_z |z - z'|} dk_\rho \quad (93)$$

the rectangular components of the magnetic field are computed using the third of equations (1) as

$$\begin{aligned} \underline{\nabla} \times \underline{\nabla} \times \underline{\pi}_x &= \underline{e}_z \frac{\partial^2 \pi_x^m}{\partial x \partial z} \\ &= \frac{-m_x \cos \phi'}{4\pi} \int_0^\infty k_\rho^2 J_1(k_\rho |\underline{\rho} - \underline{\rho}'|) e^{ik_z |z - z'|} dk_\rho \end{aligned} \quad (94)$$

From the third of equations (1) and (94), the free-space magnetic field

for this case becomes

$$\left(\frac{1}{i\omega\mu}\right) \underline{\nabla} \times \underline{\nabla} \times (-i\omega\mu\underline{\pi}^m) = -\underline{e}_z \left(\frac{m_x \cos \phi'}{4\pi}\right) \cdot \int_0^\infty k_\rho^2 J_1(k_\rho|\underline{\rho} - \underline{\rho}'|) e^{ik_z|z-z'|} dk_\rho \quad (95)$$

and from the fourth equation in (1) and (93), the electric free-space field for this case becomes

$$\underline{\nabla} \times (-i\omega\mu\underline{\pi}^m) = \underline{e}_z \left(\frac{\omega\mu m_x \sin \phi'}{4\pi}\right) \cdot \int_0^\infty \frac{k_\rho^2}{k_z} J_1(k_\rho|\underline{\rho} - \underline{\rho}'|) e^{ik_z|z-z'|} dk_\rho \quad (96)$$

The induced electric and magnetic dipole moments are

$$\begin{aligned} \begin{Bmatrix} m_x \\ m_y \\ m_z \end{Bmatrix} &= \begin{Bmatrix} \alpha_{mx} H_x^{unpert} \\ \alpha_{my} H_y^{unpert} \\ \alpha_{mz} H_z^{unpert} \end{Bmatrix} \\ \begin{Bmatrix} p_x \\ p_y \\ p_z \end{Bmatrix} &= \begin{Bmatrix} \alpha_{ex} E_x^{unpert} \\ \alpha_{ey} E_y^{unpert} \\ \alpha_{ez} E_z^{unpert} \end{Bmatrix} \end{aligned} \quad (97)$$

and **VMD**, **HMD**, **VED** and **HED** are all induced.

The  $z$ -component of the scattered field in (92) becomes

$$H_{1z}^S = \begin{Bmatrix} m_x \cos \phi' \\ p_x \sin \phi' \end{Bmatrix} \left(\frac{1}{4\pi}\right) \cdot \int_0^\infty k_\rho^2 J_1(k_\rho|\underline{\rho} - \underline{\rho}'|) F_+^{TE}(z, -d) dk_\rho \quad (98)$$

and from equations (15) and (98), the transverse components of the scattered field for the **HMD** case are given in equation (59).

The total magnetic field in region (1) for this case becomes

$$H_{\{1x,1y,1z\}}^{total} = H_{\{1x,1y,1z\}}^{incident} + H_{\{1x,1y,1z\}}^S \quad (99)$$

The  $z$ -component of the incident field above the first interface is (Kong, 1972, page 993, equation (38d))

$$\begin{aligned}
 H_{1z}^{incident} = & \left( \frac{-m_x \cos \phi}{4\pi} \right) \int_0^\infty k_\rho^2 J_1(k_\rho |\underline{\rho} - \underline{\rho}'|) \\
 & \cdot \left\{ \begin{array}{l} e^{ik_{1z}|z|} - \tilde{R}_{12}^{TE} e^{ik_{1z}(z+2d_1)} \\ -e^{ik_{1z}|z|} - \tilde{R}_{12}^{TE} e^{ik_{1z}(z+2d_1)} \end{array} \right\} dk_\rho, \quad \begin{cases} z \geq 0 \\ z < 0 \end{cases}
 \end{aligned} \tag{100}$$

and the  $z$ -component of the electric field above the first interface is from (96)

$$\begin{aligned}
 E_{1z}^{incident} = & \frac{\omega \mu m_x \sin \phi}{4\pi} \int_0^\infty \frac{k_\rho^2}{k_{1z}} J_1(k_\rho |\underline{\rho} - \underline{\rho}'|) \\
 & \cdot \left[ e^{ik_{1z}|z|} + \tilde{R}_{12}^{TM} e^{ik_{1z}(z+2d_1)} \right] dk_\rho
 \end{aligned} \tag{101}$$

From equations (15), (100) and (101), the  $\rho$ -component of the incident magnetic field is

$$\begin{aligned}
 H_{1\rho}^{incident} = & \frac{-im_x \cos \phi'}{4\pi} \int_0^\infty k_{1z} k_\rho \left[ J_0(k_\rho \rho) - \frac{J_1(k_\rho \rho)}{k_\rho \rho} \right] \\
 & \cdot \left[ e^{ik_{1z}|z|} - \tilde{R}_{12}^{TE} e^{ik_{1z}(z+2d_1)} \right] dk_\rho \\
 & \frac{-i\omega^2 \mu \varepsilon_1 m_x \cos \phi'}{4\pi} \int_0^\infty \frac{1}{k_{1z}} J_1(k_\rho \rho) \\
 & \cdot \left[ e^{ik_{1z}|z|} + \tilde{R}_{12}^{TM} e^{ik_{1z}(z+2d_1)} \right] dk_\rho
 \end{aligned} \tag{102}$$

The unperturbed fields in region 2, from equations (15) and (98)

are

$$\begin{aligned}
H_{2x}^{unpert} &= \frac{im_x \cos \phi}{4\pi} \begin{pmatrix} \cos \phi \\ \sin \phi \end{pmatrix} \int_0^\infty k_{2z} k_\rho \left[ J_0(k_\rho \rho) - \frac{J_1(k_\rho \rho)}{k_\rho \rho} \right] \\
&\quad \cdot A_2^{TE} \left[ -e^{ik_{2z}z} + \tilde{R}_{23}^{TE} e^{ik_{2z}(z+2d_2)} \right] dk_\rho \\
&\quad - \frac{i\omega^2 \mu \varepsilon_1 m_x \cos \phi}{4\pi} \begin{pmatrix} \cos \phi \\ \sin \phi \end{pmatrix} \int_0^\infty \frac{1}{k_{1z}} J_1(k_\rho \rho) \\
&\quad \cdot A_2^{TM} \left[ e^{-ik_{2z}z} + R_{23}^{TM} e^{ik_{2z}(z+2d_2)} \right] dk_\rho \\
H_{2z}^{unpert} &= \left( \frac{-m_x \cos \phi}{4\pi} \right) \int_0^\infty k_\rho^2 J_1 \left( k_\rho \sqrt{x_o^2 + y_o^2} \right) \\
&\quad \cdot A_2^{TE} \left[ e^{ik_{2z}z} - R_{23}^{TE} e^{2ik_{2z}d_2 - ik_{2z}d} \right] dk_\rho \\
E_{2x}^{unpert} &= \left( \frac{-i\omega \mu m_x \sin \phi}{4\pi} \right) \begin{pmatrix} \cos \phi \\ \sin \phi \end{pmatrix} \int_0^\infty J_1(k_\rho \rho) \\
&\quad \cdot \left[ e^{-ik_{2z}z} + R_{23}^{TE} e^{ik_{2z}(z+2d_2)} \right] dk_\rho \\
&\quad \left( \frac{i\omega \mu m_x \sin \phi}{4\pi} \right) \begin{pmatrix} \varepsilon_1 \\ \varepsilon_2 \end{pmatrix} \int_0^\infty \frac{k_{2z} k_\rho}{k_{1z}} \left[ J_0(k_\rho \rho) - \frac{J_1(k_\rho \rho)}{k_\rho \rho} \right] \\
&\quad \cdot A_2^{TM} \left[ -e^{ik_{2z}z} + R_{23}^{TM} e^{ik_{2z}(z+2d_2)} \right] dk_\rho \\
E_{2z}^{unpert} &= \frac{\omega \mu m_x \sin \phi}{4\pi} \begin{pmatrix} \varepsilon_1 \\ \varepsilon_2 \end{pmatrix} \int_0^\infty \frac{k_\rho^2}{k_{1z}} J_1 \left( k_\rho |\underline{\rho} - \underline{\rho}'| \right) \\
&\quad \cdot A_2^{TM} \left[ e^{ik_{2z}d} + R_{23}^{TM} e^{2ik_{2z}d_2 - ik_{2z}d} \right] dk_\rho
\end{aligned} \tag{103}$$

The scattered magnetic field due to the induced electric moments for this case is

$$H_{1x}^{p_{x,y,z}} \propto \begin{Bmatrix} p_x E_{2x}^{unpert} \\ p_y E_{2y}^{unpert} \end{Bmatrix}$$



$$= \frac{\omega\mu_0 m}{4\pi} \left\{ \begin{array}{l} -\alpha_{ex} \sin \phi' \\ \alpha_{ey} \cos \phi' \end{array} \right\} \frac{\omega\mu_0 m}{4\pi} \left\{ \begin{array}{l} \sin \phi \\ \cos \phi \end{array} \right\} I_8 \quad (104)$$

$$I_8 = \int_0^{\infty} J_1(k_\rho \rho) e^{-ik_{1z} z} dk_\rho$$

$$= \frac{\left[ \sqrt{x^2 + y^2 + z^2} - z \right]}{\sqrt{x^2 + y^2} \sqrt{x^2 + y^2 + z^2}} \quad (105)$$

which is negligible, because the magnetic field for this case is proportional to  $\omega^2$ .

## 6.2 An example

Assume the following

$$x_o = y_o = 0$$

$$z' = -d \quad (106)$$

$$\alpha_{mx} = \alpha_m = \alpha_{m\rho}$$

and it is easy to show

$$H_{1\rho}^S = \underline{e}_\rho \left( \frac{im\rho}{4\pi} \right) I_i$$

$$H_{1\rho}^{incident} = \underline{e}_\rho \left( \frac{im}{4\pi} \right) I_4 \quad (107)$$

$$m_\rho = \left( \frac{im}{4\pi} \right) I_6$$

so that the total field is given by

$$H_{1\rho}^{total} = \left( \frac{im}{4\pi} \right) \left[ I_4 + \left( \frac{i\alpha_{m\rho}}{4\pi} \right) I_1 I_6 \right] \quad (108)$$

which is in agreement with(85) with  $\alpha_{m\rho}$  replacing  $\alpha_{mz}$  which of course it must since the loop axis is now parallel to the x-y plane. This example provides a check on the mathematical derivations for both the **VMD** and **HMD** cases.

## 7. SCATTERED FIELDS IN REGION (1) FOR A VED IN REGION (1)

For the **VED** case, by superposition, the scattered electric fields can be written in terms of its rectangular components as the sum of three contributions, as in equation (25) as,

$$\begin{aligned} E_x^S &= E_x^v + E_x^h + E_x^m \\ E_y^S &= E_y^v + E_y^h + E_y^m \\ E_z^S &= E_z^v + E_z^h + E_z^m \end{aligned} \quad (109)$$

where  $(E_x^v, E_y^v, E_z^v)$  are the reradiated fields for the induced vertical electric dipole moment,  $(E_x^h, E_y^h, E_z^h)$  are the reradiated fields for the induced horizontal electric dipole moment, and  $(E_x^m, E_y^m, E_z^m)$  are the reradiated fields for the induced magnetic dipole moment.

Starting from the Hertz potential for a **VED** as

$$\pi_z^e = \frac{ip_e}{4\pi} \int_0^\infty \frac{k_\rho}{k_z} J_o(k_\rho |\underline{\rho} - \underline{\rho}'|) e^{-k_\rho |z-z'|} dk_\rho \quad (110)$$

the  $z$ -component of the unperturbed electric field is given by

$$\begin{aligned} E_z &= \frac{1}{-i\omega\varepsilon} \left( \frac{\partial^2}{\partial z^2} + k_o^2 \right) (p_e \pi_z^e), \quad p_e = Il \\ &= \left( \frac{i}{4\pi} \right) \left( \frac{p_e}{-i\omega\varepsilon} \right) \int_0^\infty (k_o^2 - k_\rho^2) \frac{k_\rho}{k_z} J_o(k_\rho |\underline{\rho} - \underline{\rho}'|) e^{-k_z |z-z'|} dk_\rho \\ &= \left( \frac{-ip_e}{4\pi\omega\varepsilon} \right) \int_0^\infty \frac{k_\rho^3}{k_z} J_o(k_\rho |\underline{\rho} - \underline{\rho}'|) e^{-k_z |z-z'|} dk_\rho \end{aligned} \quad (111)$$

The unperturbed transverse components are from equation (15)

$$\begin{aligned} \underline{E}_t &= \frac{e_\rho}{k_\rho^2} \frac{\partial^2 E_z}{\partial \rho \partial z} \\ &= \left( \frac{\pm ip_e}{4\pi\omega\varepsilon} \right) (\underline{e}_x \cos \phi + \underline{e}_y \sin \phi) \\ &\quad \cdot \int_0^\infty k_\rho^2 J_1(k_\rho |\underline{\rho} - \underline{\rho}'|) e^{-k_z |z-z'|} dk_\rho, \quad \begin{cases} z > z' \\ z < z' \end{cases} \end{aligned} \quad (112)$$

The unperturbed fields from a **HED** are generated by a Hertzian dipole given by

$$\pi_x^e = \left( \frac{ip_x}{4\pi} \right) \int_0^\infty \frac{k_\rho}{k_z} J_0(k_\rho |\underline{\rho} - \underline{\rho}'|) e^{ik_z |z - z'|} dk_\rho \quad (113)$$

and from equation (1), the  $z$ -component of the electric field is

$$\begin{aligned} \underline{E} &= \frac{1}{-i\omega\varepsilon} (\nabla \times \nabla \times \pi_x^e) \\ &= \left( \frac{+ip_x}{4\pi\omega\varepsilon} \right) \int_0^\infty k_\rho^2 J_1(k_\rho |\underline{\rho} - \underline{\rho}'|) e^{ik_z |z - z'|} dk_\rho, \quad \begin{cases} z > z' \\ z < z' \end{cases} \end{aligned} \quad (114)$$

the  $z$ -component and transverse components for a **HED** are (Kong, 1972, p.993, equation (37a))

$$E_z = \frac{-ip_x \cos \phi'}{4\pi\omega\varepsilon} \int_0^\infty k_\rho^2 J_1(k_\rho |\underline{\rho} - \underline{\rho}'|) e^{ik_z |z - z'|} dk_\rho \quad (115)$$

and

$$E_\rho = \frac{-p_x \cos \phi'}{4\pi\omega\varepsilon} \int_0^\infty k_z k_\rho \left[ J_0(k_\rho |\underline{\rho} - \underline{\rho}'|) - \frac{J_1(k_\rho |\underline{\rho} - \underline{\rho}'|)}{k_\rho |\underline{\rho} - \underline{\rho}'|} \right] e^{ik_\rho |z - z'|} dk_\rho \quad (116)$$

The unperturbed electric fields from an induced **HMD** are generated by a horizontal Hertz potential

$$\pi_x^m = \left( \frac{im_x}{4\pi} \right) \int_0^\infty \frac{k_\rho}{k_z} J_0(k_\rho |\underline{\rho} - \underline{\rho}'|) e^{ik_z |z - z'|} dk_\rho \quad (117)$$

and from equation (1) the  $z$ -component of the electric field is (Kong, 1972, p.993, equation (38a))

$$\begin{aligned} \underline{E}_z &= \nabla \times \underline{\pi}_x^m \\ &= \left( \frac{\omega\mu_o m_x \sin \phi'}{4\pi} \right) \int_0^\infty \frac{k_\rho^2}{k_z} J_1(k_\rho |\underline{\rho} - \underline{\rho}'|) e^{ik_z |z - z'|} dk_\rho \end{aligned} \quad (118)$$

and the transverse components for the **HMD** are given by (Kong, 1972, p.993, equation (38a))

$$\begin{aligned} \underline{E}_\rho &= \frac{\underline{e}_\rho}{k_\rho^2} \frac{\partial^2 E_z}{\partial \rho \partial z} \\ E_y^x &= \left( \frac{i\omega\mu_o m_x \sin \phi'}{4\pi} \right) \begin{pmatrix} \cos \phi \\ \sin \phi \end{pmatrix} \\ &\cdot \int_0^\infty k_\rho \left[ J_o(k_\rho |\underline{\rho} - \underline{\rho}'|) - \frac{J_1(k_\rho |\underline{\rho} - \underline{\rho}'|)}{k_\rho |\underline{\rho} - \underline{\rho}'|} \right] e^{ik_\rho |z - z'|} dk_\rho \end{aligned} \quad (119)$$

The  $z$ -component of the total electric field for a **VED** in region 1, is given by

$$E_{1z}^{total}(\rho, z) = \left( \frac{-IA}{4\pi\omega\varepsilon_1} \right) \left[ I_9 + \left( \frac{i \left( \frac{\alpha_{ez}}{\varepsilon_0} \right)}{4\pi} \right) I_{10} I_{11} \right] \quad (120)$$

which is the dual result of equation (85), with the exception that the TE coefficients are replaced by the TM coefficients in the following integrals

$$\begin{aligned} I_9 &= \int_0^\infty \frac{k_\rho^3}{k_{1z}} J_0 \left( k_\rho \sqrt{x^2 + y^2} \right) \\ &\cdot \left[ e^{ik_{1z}|z|} + R_{12}^{TM} e^{ik_{1z}(z+2k_1)} \right] dk_\rho \end{aligned} \quad (121)$$

$$\begin{aligned} I_{10} &= \int_0^\infty \frac{k_\rho^3}{k_{2z}} J_0 \left( k_\rho \sqrt{(x - x_o)^2 + (y - y_o)^2} \right) F_+^{TM}(z, -d) dk_\rho \\ F_+^{TM}(z, -d) &= T_{21}^{TM} B_2^{TM} e^{ik_{1z}(z+d_1)} e^{-ik_{2z}d_1} \\ B_2^{TM} &= \frac{e^{ik_{2z}d} - R_{23}^{TM} e^{ik_{2z}(2d_2-d)}}{1 + R_{12}^{TM} R_{23}^{TM} e^{2ik_{2z}(d_2-d_1)}} \end{aligned} \quad (122)$$

$$\begin{aligned}
 I_{11} &= \int_0^{\infty} \frac{k_{\rho}^3}{k_{1z}} J_0 \left( k_{\rho} \sqrt{x_o^2 + y_o^2} \right) A_2^{TM} \\
 &\quad \cdot \left[ e^{-ik_{2z}z} + R_{23}^{TM} e^{ik_{2z}(z+2d_2)} \right] dk_{\rho} \quad (123) \\
 A_2^{TM} &= \frac{T_{12}^{TM} e^{i(k_{1z}-k_{2z})d_1}}{1 + R_{12}^{TM} R_{23}^{TM} e^{2ik_{2z}(d_2-d_1)}}
 \end{aligned}$$

## 8. SCATTERED FIELDS IN REGION (1) FOR A HED IN REGION (1).

For the **HED** case, by superposition, the scattered electric fields can be written in terms of rectangular in a form similar to equation (89) as

$$\begin{aligned}
 E_x^S &= E_x^{m_x} + E_x^{m_y} + E_x^{m_z} + E_x^{p_x} + E_x^{p_y} + E_x^{p_z} \\
 E_y^S &= E_y^{m_x} + E_y^{m_y} + E_y^{m_z} + E_y^{p_x} + E_y^{p_y} + E_y^{p_z} \quad (124) \\
 E_z^S &= E_z^{m_x} + E_z^{m_y} + E_z^{m_z} + E_z^{p_x} + E_z^{p_y} + E_z^{p_z}
 \end{aligned}$$

where  $\underline{E}^{m_{x,y,z}}$  is the radiated field from the induced magnetic dipole moments and  $\underline{E}^{p_{x,y,z}}$  is the radiated field from the induced electric dipole moments.

Starting with the Hertz potential for a **HED** in the  $\rho$ -direction as

$$\pi_x^e = \frac{ip_x}{4\pi} \int_0^{\infty} \frac{k_{\rho}}{k_z} J_0 \left( k_{\rho} |\underline{\rho} - \underline{\rho}'| \right) e^{ik_z |z - z'|} dk_{\rho} \quad (125)$$

the rectangular components of the electric and magnetic field are, using the first and second of equations (1), given by

$$\begin{aligned}
 \underline{E} &= \left( \frac{1}{i\omega\epsilon} \right) \underline{\nabla} \times \underline{\nabla} \times (p_e \pi_x^e) \\
 \underline{H} &= \underline{\nabla} \times (p_e \pi_x^e) \quad (125)
 \end{aligned}$$

The unperturbed fields are

$$p_e = Il \quad (126)$$

$$\begin{aligned}
 E_{2z}^{unpert} &= \left( \frac{ip_x \cos \phi'}{4\pi\omega\epsilon_2} \right) \int_0^\infty k_\rho^2 J_1 \left( k_\rho \sqrt{x_o^2 + y_o^2} \right) \\
 &\quad \cdot B_2^{TM} \left[ e^{ik_{2z}z} + R_{21}^{TM} e^{-ik_{2z}(z+2d_2)} \right] \\
 H_{2z}^{unpert} &= \left( \frac{ip_x \sin \phi'}{4\pi} \right) \int_0^\infty \frac{k_\rho^2}{k_{2z}} J_1 \left( k_\rho \sqrt{x_o^2 + y_o^2} \right) \\
 &\quad \cdot B_2^{TE} \left[ e^{ik_{2z}d} + R_{23}^{TE} e^{-ik_{2z}(z+2d_1)} \right]
 \end{aligned} \tag{127}$$

The scattered field are obtained from equation (100) by duality; i.e.,

$$\begin{aligned}
 \underline{H}^s &\rightarrow \underline{E}^s \\
 \underline{E}^s &\rightarrow \underline{H}^s
 \end{aligned} \tag{128}$$

## 9. METAL DETECTOR ANALYSIS

One type of metal detector uses a single transmitting loop and four receiving loops as shown in figure 7 (Hill and Cavcey, 1987). The detector sums the output of the four loops, but two of the polarities are reversed. Because of the detector symmetry, the direct of the transmitting loop produces a zero output. Hence the desired nulling of the strong direct field is achieved.

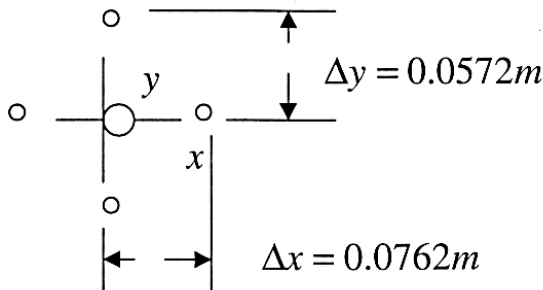


**Figure 7.** Geometry for a metal detector with a central transmitting loop and four receiving loops.

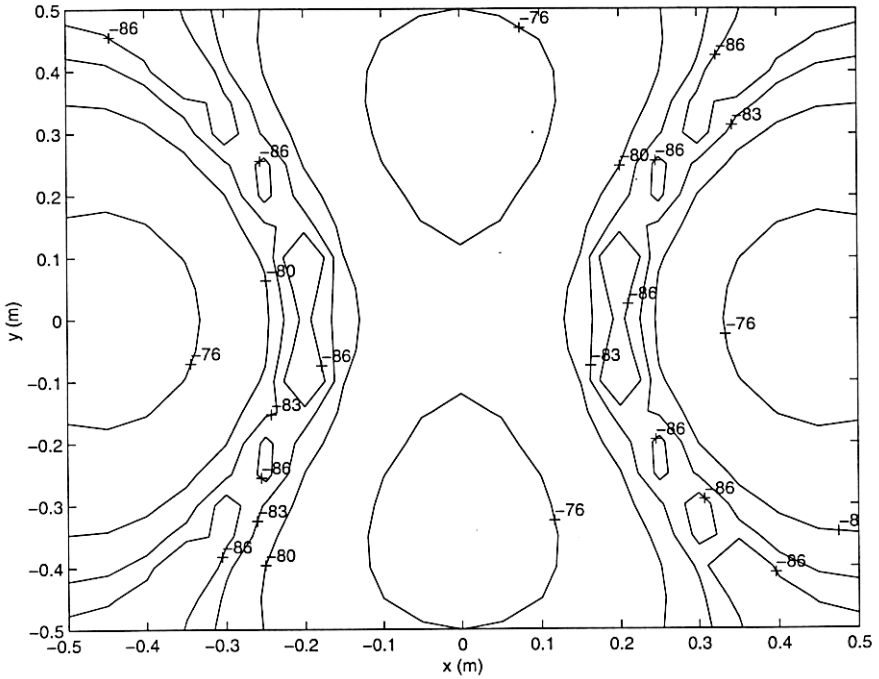


**Figure 8.** Contour plot of  $|V_r(x, y)|$  for a metal detector response from a perfectly conducting sphere.

The total received voltage can be written

$$v_r = (i\omega\mu NA)(H_{z1}^S - H_{z2}^S + H_{z3}^S - H_{z4}^S) \quad (129)$$

where  $N$  is the number of turns.

Figure 8 shows a contour plot of the magnitude of the received voltage in equation (127) versus  $x$  and  $y$  for a perfectly conducting sphere buried 50 cm below the interface in “sandy soil”.

The parameters for the plot in figure 8 are given in Table V.

Parameter	Value
Frequency	3KHz
D	0.5m
Sphere Radius	0.0005m
$\sigma_1$	0.01 Mho/m
$\varepsilon_1$	10.
$\sigma_2$	0.05 Mho/m
$\varepsilon_2$	20.
$d_2$	1 m

**Table V.** Parameter values for metal detector example

## ACKNOWLEDGMENT

The Editor thanks K. A. Michalski and one anonymous Reviewer for reviewing the paper.

## REFERENCES

1. Baños, A., *Dipole Radiation in the Presence of a Conducting Half-Space*, Pergamon Press, 1966.
2. Barrick, D. E., "Non-Sinusoidal Coastal ELF ASW Radar, Final Report on SBIR Phase 1 Topic Number N93-227", Naval Air Systems Command PMA-264, Contract Number N00019-94-C-0102, December, 1995.
3. Chew, W. C., "Waves and Fields in Inhomogeneous-Media," *IEEE Press Series on Electromagnetic Waves*, 1995.
4. Collin, R. E., *Field Theory of Guided Waves*, McGraw-Hill, New York, 1960.
5. Fraser-Smith, A. C., D. M. Bubenik, and O. G. Villard, Jr., "Large-amplitude changes induced by a Seabed in the sub-LF electromagnetic fields produced in, on, and above the sea by harmonic dipole sources," *Radio Science*, Vol. 22, No. 4, 567-577, July-August, 1987.
6. Fraser-Smith, A. C., and E. M. Bubenik, "Compendium of the ULF/ ELF electromagnetic fields generated above a sea of finite depth by submerged harmonic dipoles," Stanford Electronics Laboratories, Department of Electrical Engineering, Stanford University, Stanford, CA 94305, Technical Report E715-1, January, 1980, Sponsored by ONR, Contract NO. N00014-77-C-0292.



7. Gröbner, W. Und N. Hofreiter, *Intgraltafel, Zweiter Teil, Bestimmte Integrale*, Springer-Verlag, 1961.
8. Harrington, R. F., *Time-Harmonic Electromagnetic Fields*, McGraw-Hill, New York, 1961.
9. Hill, D. A., and K. H. Cavcey, "Coupling between two antennas separated by a planar interface," *IEEE Transactions on Geoscience and Remote Sensing*, Vol. GE-25, No. 4, 422–430, July, 1987.
10. Hill, D. A., and J. R. Wait, "The electromagnetic response of a buried sphere for buried-dipole excitation," *Radio Science*, Vol. 8, No. 8–9, 813–818, August-September, 1973.
11. Ishimaru, A., *Electromagnetic Wave Propagation, Radiation, and Scattering*, Prentice Hall, Englewood Cliffs, New Jersey, 1991.
12. Kern, D. M., *Plane-Wave Scattering-Matrix Theory of Antennas, and Antenna-Antenna Interactions*, U. S. Department of Commerce, National Bureau of Standards (now the National Institute of Science and Technology), June, 1981.
13. Kong, J. A., "Electromagnetic Fields Due to Dipole Antennas Over Stratified Anisotropic Media," *Geophysics*, Vol. 37, No. 6, 985–996, December, 1972.
14. Ott, R. H., "Electromagnetic scattering by buried objects in the HF/VHF/UHF frequency bands," *Progress in electromagnetics Research*, PIER 12, 371–419, 1996.
15. Ott, R. H., "The Plane-Wave Scattering Matrix (PWSM) formulation for three interfaces plus a scatterer," submitted to *Progress in Electromagnetic Research*, 1998.
16. Sommerfeld, A., *Partial Differential Equations in Physics*, Academic Press Inc., New York, 1949.
17. Stratton, J. A., *Electromagnetic Theory*, McGraw-Hill, New York, 1941.
18. Wait, J. R., "The magnetic dipole over the horizontally stratified earth," *Canadian Journal of Physics*, Vol. 29, 577–592, 1951.
19. Wait, J. R., "On the electromagnetic response of a conducting sphere to a dipole field," *Geophysics*, Vol. 25, No. 3, 649–658, 1960.
20. Wait, J. R., "Electromagnetic induction in a small conducting sphere above a resistive half-space," *Radio Science*, Vol. 3 (New Series), No. 10, 1030–1034, October, 1968.
21. Van De Hulst, H. C., *Light Scattering by Small Particles*, Dover Publications, New York, 1957.